

Scalable Capacity Bounding Models for Wireless Networks

Jinfeng Du, *Member, IEEE*, Muriel Médard, *Fellow, IEEE*, Ming Xiao, *Senior Member, IEEE*,
and Mikael Skoglund, *Senior Member, IEEE*

Abstract—The framework of network equivalence theory developed by Koetter et al. introduces a notion of channel emulation to construct noiseless networks as upper (resp. lower) bounding models, which can be used to calculate the outer (resp. inner) bounds for the capacity region of the original noisy network. Based on the network equivalence framework, this paper presents scalable upper and lower bounding models for wireless networks with potentially many nodes. A channel decoupling method is proposed to decompose wireless networks into decoupled multiple-access channels (MACs) and broadcast channels (BCs). The upper bounding model, consisting of only point-to-point bit pipes, is constructed by firstly extending the “one-shot” upper bounding models developed by Calmon et al. and then integrating them with network equivalence tools. The lower bounding model, consisting of both point-to-point and point-to-points bit pipes, is constructed based on a two-step update of the lower bounding models to incorporate the broadcast nature of wireless transmission. The main advantages of the proposed methods are their simplicity and the fact that they can be extended easily to large networks with a complexity that grows linearly with the number of nodes. It is demonstrated that the resulting upper and lower bounds can approach the capacity in some setups.

Index Terms—capacity, channel decoupling, channel emulation, equivalence, wireless networks

I. INTRODUCTION

A theory of network equivalence has been established in [1], [2] by Koetter et al. to characterize the capacity of a (large) memoryless noisy network. The original noisy network is first decomposed into many independent single-hop noisy channels, each of which is then replaced by the corresponding upper (resp. lower) bounding model consisting of only noiseless bit pipes. The capacity region of the resulting noiseless network serves as an outer (resp. inner) bound for the capacity region

This work was presented in part at the IEEE International Symposium on Information Theory in July 2013 and in July 2014. This work was funded in part by the Swedish Research Council (VR) and by the Air Force Office of Scientific Research (AFOSR) under award No. FA9550-09-1-0196 and FA9550-13-1-0023.

Jinfeng Du is with Research Lab of Electronics, Massachusetts Institute of Technology, Cambridge, MA, USA (Email: jinfeng@mit.edu). He was with School of Electrical Engineering, Royal Institute of Technology, Stockholm, Sweden.

Muriel Médard is with Research Lab of Electronics, Massachusetts Institute of Technology, Cambridge, MA, USA (Email: medard@mit.edu).

Ming Xiao and Mikael Skoglund are with School of Electrical Engineering and the ACCESS Linnaeus Center, Royal Institute of Technology, Stockholm, Sweden (Email: {mingx, skoglund}@kth.se).

Copyright (c) 2014 IEEE. Personal use of this material is permitted. However, permission to use this material for any other purposes must be obtained from the IEEE by sending a request to pubs-permissions@ieee.org.

of the original noisy network, whose capacity is otherwise difficult to characterize. A noisy channel and a noiseless bit pipe are said to be equivalent if the capacity region of any arbitrary network that contains the noisy channel remains unchanged after replacing the noisy channel by its noiseless counterpart. The equivalence between a point-to-point noisy channel and a point-to-point noiseless bit pipe has been established in [1] as long as the rate of the latter equals the capacity of the former. For independent single-hop multi-terminal channels, such as the multiple-access channel (MAC), the broadcast channel (BC), and the interference channel (IC), operational frameworks for constructing upper and lower bounding models have been proposed in [2]. The constructive proofs presented in [1], [2] are based on a notion of channel emulation over a stacked replicas of the channel, where the lower bounding models are established based on channel coding arguments and the upper bounding models are constructed based on lossy source coding arguments.

The bounding accuracy, in terms of both multiplicative and additive gaps between capacity upper and lower bounds, has been outlined in [2] for general noisy networks. Explicit upper and lower bounding models for MAC/BC/IC with two sources and/or two destinations have been constructed in [2]–[4]. For networks consisting of only point-to-point channels, MACs with two transmitters, and BCs with two receivers, the additive gap for Gaussian networks and the multiplicative gap for binary networks have been specified in [3]. The bounds obtained from network equivalence tools [2]–[4] can be tight in some setups, as shown in [4] for a multiple unicast network consisting of noisy two-user BCs, and in [5] for a frequency-division AWGN relay network in the wideband regime when the BC is physically degraded or when the source treats the stochastically degraded BC as physically degraded. A class of “one-shot” upper bounding models proposed in [6] by Calmon et al. introduces an auxiliary node for each BC/MAC to facilitate separate characterization of the sum rate and the individual rates. The rate of a bit pipe from/to the auxiliary node can be characterized either by channel emulation over infinite number of channel uses as in [1], [2], or by emulating the transmission over each channel use (hence named “one-shot”).

Although it has been established in [7] that separate source and channel coding incurs no capacity loss in transmitting a memoryless source over a memoryless point-to-point channel, similar separation results on memoryless networks are not known until recently. The optimality of channel and network coding separation for general communication demands over

networks consisting of independent memoryless point-to-point channels is established in [1] based on the network equivalence theory, where the networks may be cyclic or acyclic and alphabets can be discrete or continuous. Feedback and cooperation among nodes are also accommodated, but the sources have to be independent. For single-source multicast connections over networks consisting of point-to-point discrete memoryless channels (DMCs) with finite alphabets, separation of channel and network coding has been established in [8] for acyclic synchronized networks and in [9] for asynchronous networks with and without cycles. While both [8] and [9] rely on the max-flow min-cut theorem [10] to show the converse (cf. upper bounding model), similar results on channel-network separation have been established in [11] by using normalized entropy vectors. For point-to-point channels, the same upper bounding models established in [1] have also been developed in [12] for DMCs with finite-alphabet, and in [13] under the notion of strong coordination, where total variation (i.e., an additive gap) is used to measure the difference between the desired joint distribution and the empirical joint distribution of a pair of sequences (or a pair of symbols as in *empirical coordination*). The concept of channel emulation [1], [2], on the other hand, focuses on the set of jointly typical input-output pairs and the difference between the empirical joint distribution (averaged over ensembles of channel emulators) and the desired joint distribution is quantified by a multiplicative gap to ensure a small probability of error events¹. As we focus on characterizing capacity (bounds) rather than reconstructing (exact) common randomness for multi-terminal channels, we shall follow the channel emulation framework [1], [2] when constructing bounding models for BCs and MACs.

It is, however, non-trivial to apply the network equivalence tools [1]–[4] onto wireless networks owing to the broadcast nature of wireless transmission. On one hand, the bounding models proposed in [2] for MACs/BCs with m transmitters/receivers contain up to $(2^m - 1)$ bit pipes, leading to computational inefficiency when m is large (as in a wireless hotspot which may contain potentially many users). On the other hand, the received signal at a terminal may contain several broadcasted signals, which creates dependence/interference among several transmitter-receiver pairs. Although such dependence has been partially incorporated into ICs, the whole family of non-layered multi-hop channels (e.g., relay channels) have been excluded from consideration since the channel emulation techniques are developed for single-hop channels.

In this paper, we present simple but efficient methods to construct upper and lower bounding models for wireless networks with potentially many nodes, at a complexity that grows linearly with the number of nodes. We propose a channel decoupling approach to decompose a memoryless wireless network into decoupled BCs and MACs. In our bounding models, the constraints on the sum rate and on the individual rates are characterized by different channel emulation techniques as inspired by [6]. Our upper bounding models, which consist of only point-to-point bit pipes, are constructed by first

extending the one-shot models for MACs/BCs to many-user scenarios and then integrating them with the channel emulation techniques. Our lower bounding models, which contain both point-to-point and point-to-points (hyper-arc) bit pipes, are obtained based on a two-step update of the decoupled BCs and MACs by taking their dependence into account. The main advantage of our proposed bounding models are their simplicity and the fact that they can be easily extended to large networks. We demonstrate by examples that the resulting upper and lower bounds can approach the capacity in some setups.

Throughout this paper, we assume memoryless independent sources as in [1], where the optimality of channel-network separation is established for networks with only point-to-point channels. Extension to memoryless correlated sources can be found in [14], [15] where channel-network separation is established in the context of lossy [14], [15] and lossless [15] source coding problems over networks with only point-to-point DMCs. Extension to AWGN channels is also established in [15]. We also assume that the distortion components (e.g., noise) are independent from the transmitted signals. This assumption can be relaxed in scenarios where the noise power is dependent on the power of input signals, and in such scenarios we take the smallest (resp. largest) noise power when constructing upper (resp. lower) bounding models. We further assume that the distortion components at receiving nodes within a coupled² BC are mutually independent³, and the scenario of coupled BC with correlated noise will be investigated in our future work. Note that in this paper our focus is on constructing noiseless bounding networks that can serve as a basis to compute capacity bounds, rather than finding the capacity of a noiseless network, which itself is a very difficult problem [16], [17]. We refer to [18]–[24] for various computational tools available to characterize (bounds on) the capacity of noiseless networks.

There are some other methods aiming at characterizing the capacity of wireless networks. A deterministic approach proposed in [25] can approximate the capacity of Gaussian networks within a constant gap in the high signal-to-noise ratio (SNR) regime, where amplify-and-forward (AF) has been proved to approach the capacity in multi-hop layered networks [26]. A layering approach with a global information routing proposed in [27] for wireless networks with non-coupled BCs and MACs can provide lower bounds within a multiplicative gap from the capacity upper bound. Capacity approximations for multiple unicast transmissions over coupled wireless networks developed in [28] combines polymatroidal network analysis with carefully designed coding schemes for each independent single-hop interference channel, and the approximation accuracy is characterized for bidirectional networks with symmetric fading coefficients. Since we aim at approaches that can be used in all SNR regions and for all communication tasks, we do not follow the methods developed in [25]–[28].

²The definition of coupled and non-coupled networks will be introduced in Sec. II-A.

³Though we still allow noise correlation at receiving nodes within a non-coupled BC.

¹Jointly typical pairs with decoding error probability larger than a threshold [1] are expurgated from channel emulators.

The rest of this work is organized as follows. We first introduce in Sec. II a few important definitions and a brief introduction of the network equivalence theory and the one-shot method. Then in Sec. III we present our improvement on the bounding models for independent BCs and MACs. In Sec. IV we describe the network decoupling method for coupled networks and demonstrate how the upper and lower bounding models are constructed by taking the coupled structure into account. We illustrate our bounding models in Sec. V by constructing upper and lower bounding models for coupled networks and conclude this work in Sec. VI.

II. NETWORK EQUIVALENCE THEORY AND THE ONE-SHOT BOUNDING METHOD

In this section we present a few basic definitions that are frequently used in our paper and give a brief introduction of the stacked as well as the one-shot channel emulation techniques. We inherit the setups for bounding models and channel emulation arguments from [1], [2], but our notation is slightly different to minimize the number of sub-/sup-scripts. X represents a random variable drawn from an alphabet \mathcal{X} with cardinality $|\mathcal{X}|$, and x is a realization with probability $p(x) \triangleq p_X(X=x)$. We use subscripts (X_i, x_i) to differentiate random variables and use superscripts (x^N) to indicate the number of realizations drawn independently from the same random variable. $X_{[1:n]}$ refers to $\{X_1, X_2, \dots, X_n\}$ and $x_{[1:n]}$ is the corresponding set of realizations, one from each random variable. We use $p(\mathbf{y}|\mathbf{x})$ to represent the transition function of a memoryless network where \mathbf{x} is a vector containing one realization from every channel input alphabet and \mathbf{y} is the vector for all channel outputs. The dimension of \mathbf{x} and \mathbf{y} depends on the specific network and therefore will not be specified unless necessary.

A. Basic Definitions

We represent a memoryless channel/network by a triplet consisting of the input alphabets, the output alphabets, and a conditional probability distribution (i.e., the transition function) that can fully characterize its behavior⁴. A point-to-point memoryless channel with input alphabet \mathcal{X}_i , output alphabet \mathcal{Y}_j , and transition probability $p(y_j|x_i)$ is therefore denoted by

$$\mathcal{N}_{i \rightarrow j} \triangleq (\mathcal{X}_i, p(y_j|x_i), \mathcal{Y}_j).$$

In wireless networks, a node may receive signals from multiple transmitters via MAC or parallel channels, and/or transmit to multiple receivers via BC or parallel channels. Therefore a node may associate with multiple input/output alphabets. For a given node v , letting I_v be the number of its incoming parallel channels and O_v be the number of its outgoing parallel channels, we denote the alphabets associated with its outgoing channels by the Cartesian product $\mathcal{X}_v \triangleq \prod_{i=1}^{O_v} \mathcal{X}_{v,i}$ and the alphabets associated with its incoming channels by $\mathcal{Y}_v \triangleq \prod_{j=1}^{I_v} \mathcal{Y}_{v,j}$. A memoryless network \mathcal{N}_T with the set

of nodes T and the transition function $p(\mathbf{y}|\mathbf{x})$ can be fully represented as

$$\mathcal{N}_T \triangleq \left(\prod_{v \in T} \mathcal{X}_v, p(\mathbf{y}|\mathbf{x}), \prod_{v \in T} \mathcal{Y}_v \right) \quad (1)$$

$$= \left(\prod_{v \in T} \prod_{i=1}^{O_v} \mathcal{X}_{v,i}, p(\mathbf{y}|\mathbf{x}), \prod_{v \in T} \prod_{j=1}^{I_v} \mathcal{Y}_{v,j} \right) \quad (2)$$

$$= \left(\prod_n \mathcal{X}_n, p(\mathbf{y}|\mathbf{x}), \prod_m \mathcal{Y}_m \right). \quad (3)$$

Note that the structure and behavior of a memoryless network are explicitly characterized by the triplet in (2), which specifies the association of input/output alphabet(s) to a specific node in the network. The triplet in (3), on the other hand, focuses on each individual channel/sub-network and highlights its associated input/output alphabets, where the underlying network structure is implicitly assumed. Unless necessary, hereafter we will focus on the model (3) without specifying \mathcal{X}_n as the solo alphabet of a node or as one of its outgoing alphabets.

Definition 1 (Independent Channel): A point-to-point channel $\mathcal{N}_{i \rightarrow j} = (\mathcal{X}_i, p(y_j|x_i), \mathcal{Y}_j)$ within a memoryless network $\mathcal{N}_T = (\prod_n \mathcal{X}_n, p(\mathbf{y}|\mathbf{x}), \prod_m \mathcal{Y}_m)$ is said to be independent if the network transition function $p(\mathbf{y}|\mathbf{x})$ can be partitioned as

$$p(\mathbf{y}|\mathbf{x}) = p(\mathbf{y}_{/j}|\mathbf{x}_{/i})p(y_j|x_i), \quad (4)$$

where $\mathbf{x}_{/i}$ denotes the vector of \mathbf{x} without element x_i , and similarly for $\mathbf{y}_{/j}$.

To highlight the independence, we emphasize the notation for network \mathcal{N}_T as

$$\begin{aligned} \mathcal{N}_T &= \mathcal{N}_{i \rightarrow j} \times \mathcal{N}_{T/(i \rightarrow j)} \quad (5) \\ &\triangleq (\mathcal{X}_i, p(y_j|x_i), \mathcal{Y}_j) \times \left(\prod_{n \neq i} \mathcal{X}_n, p(\mathbf{y}_{/j}|\mathbf{x}_{/i}), \prod_{m \neq j} \mathcal{Y}_m \right). \end{aligned}$$

A sub-network $\mathcal{N}_{S \rightarrow D} \triangleq (\prod_{n \in S} \mathcal{X}_n, p(\mathbf{y}_D|\mathbf{x}_S), \prod_{m \in D} \mathcal{Y}_m)$ within \mathcal{N}_T is said to be independent, denoted by

$$\mathcal{N}_T = \mathcal{N}_{S \rightarrow D} \times \mathcal{N}_{T/(S \rightarrow D)}, \quad (6)$$

if the network transition probability can be partitioned as

$$p(\mathbf{y}|\mathbf{x}) = p(\mathbf{y}_D|\mathbf{x}_S)p(\mathbf{y}_{/D}|\mathbf{x}_{/S}). \quad (7)$$

An independent sub-network may be further partitioned into several independent channels and/or sub-networks.

Definition 2 (Coupled/Non-coupled Network): A network is said to be coupled if any of its channels is part of a MAC and a BC simultaneously. That is, it contains a sub-network $\mathcal{N}_{S \rightarrow D}$ with $|S| \geq 2$, $|D| \geq 2$, and its transition function $p(\mathbf{y}_D|\mathbf{x}_S)$ can't be partitioned into non-trivial product format. Otherwise, the network is non-coupled. A MAC and a BC are said to be coupled if they share a common link.

For example, the classical three-node relay channel $p(y, y_1|x, x_1)$ is coupled and the two-hop diamond network is non-coupled. Wireless networks, as expected, are in general coupled owing to the broadcast nature of microwave propagation.

Definition 3 (Bit pipe): A point-to-point bit pipe of rate $R \geq 0$ is a noiseless channel that can reliably transmit $\lfloor nR \rfloor$

⁴As in [1], [2], we only focus on channels/networks where the transition functions exist.

bits during n channel uses for any positive integer n . It is represented as

$$\mathcal{C}_{i \rightarrow j} = (\{0, 1\}^{\lfloor nR \rfloor}, \delta(y_j - x_i), \{0, 1\}^{\lfloor nR \rfloor}), \forall n \geq 1,$$

where $\delta(\cdot)$ is the Kronecker delta function. A point-to-point bit pipe (hyper-arc) is denoted by

$$\mathcal{C}_{i \rightarrow J} = (\{0, 1\}^{\lfloor nR \rfloor}, \prod_{j \in J} \delta(y_j - x_i), \prod_{j \in J} \{0, 1\}^{\lfloor nR \rfloor}), \forall n \geq 1,$$

where $|J|$ is the number of heads of this hyper-arc.

Definition 4 (Capacity Bounding Models [1]): Given two independent (multi-terminal) channels \mathcal{C} and \mathcal{N} , \mathcal{C} is said to upper bound \mathcal{N} , or equivalently \mathcal{N} lower bounds \mathcal{C} , if the capacity (region) of $\mathcal{N} \times \mathcal{W}$ is a subset of that for $\mathcal{C} \times \mathcal{W}$ for any network \mathcal{W} . We denote their relationship by $\mathcal{N} \subseteq \mathcal{C}$. \mathcal{C} and \mathcal{N} are said to be equivalent if $\mathcal{C} \subseteq \mathcal{N} \subseteq \mathcal{C}$.

For an independent noisy channel \mathcal{N} , we construct channels \mathcal{C}_u and \mathcal{C}_l consisting of only noiseless bit pipes, such that \mathcal{C}_u is the upper bounding model and \mathcal{C}_l is the lower bounding model for \mathcal{N} , i.e.,

$$\mathcal{C}_l \subseteq \mathcal{N} \subseteq \mathcal{C}_u. \quad (8)$$

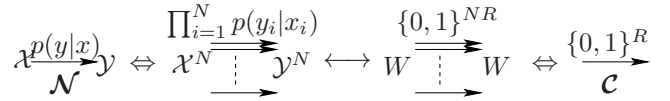
B. Network Equivalence Theory for Independent Channels

In [1], the equivalence between an independent point-to-point noisy channel \mathcal{N} and a noiseless point-to-point bit pipe \mathcal{C} has been established, as long as the with capacity of \mathcal{N} equals the rate of \mathcal{C} , by showing that any code that runs reliably on a network $\mathcal{N} \times \mathcal{W}$ can also operate on $\mathcal{C} \times \mathcal{W}$ with asymptotically vanishing error probability. The argument is based on a channel emulation technique over a stacked network where N parallel replicas of the network have been put together to run the code. As illustrated in Fig. 1, for noisy \mathcal{N} with capacity C and rate- R bit pipe \mathcal{C} , the proof can be divided into three steps.

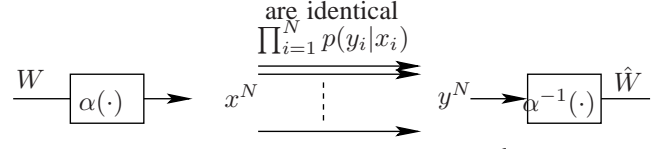
In Step I, a network and its N -fold stacked network (consisting of N parallel replicas of the network) are proved to share the same rate region by showing that any code that can run on the network can also run on its stacked network, and vice versa. Therefore we only need to show the equivalence between the stacked network for \mathcal{N} and that for \mathcal{C} , as illustrated in Fig. 1(a).

In Step II, the proof of $\mathcal{C} \subseteq \mathcal{N}$ employs a channel coding argument over the stack of N channel replicas as illustrated in Fig. 1(b): A message W of 2^{NR} bits is mapped by the channel encoder $\alpha(\cdot)$ onto a codeword x^N of length N , and then transmitted over the N -stack noisy channels, with one symbol on each replica, such that reliable transmission over the noisy stacked network can be realized with arbitrary small error probability as N goes to infinity for all $R < C$.

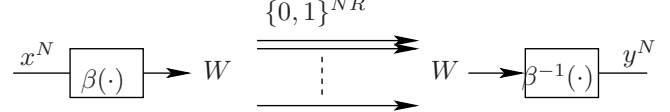
In Step III, the proof of $\mathcal{N} \subseteq \mathcal{C}$ is based on a lossy source coding argument as illustrated in Fig. 1(c): The input sequence x^N to the noisy stacked network is first quantized/compressed by a lossy source encoder $\beta(\cdot)$ into 2^{NR} bits, represented by the message W , which is then transmitted through the noiseless stacked network. The reconstructed sequence y^N is selected in such a way that it is jointly typical with the transmitted sequence x^N , in contrast to the usual distortion



(a) Capacity regions of a network and its stacked network



(b) Channel coding argument to prove $\mathcal{C} \subseteq \mathcal{N}$ for all $R < C$



(c) Lossy source coding argument to prove $\mathcal{N} \subseteq \mathcal{C}$ for all $R > C$

Fig. 1. A point-to-point noisy channel $\mathcal{N} = (\mathcal{X}, p(y|x), \mathcal{Y})$ with capacity $C = \max_{p(x)} I(X; Y)$ and a noiseless point-to-point bit pipe \mathcal{C} of rate R are said to be equivalent if $R = C$, where the equality comes from the continuity of the capacity region. The input/output of their corresponding stacked networks are $x^N \in \mathcal{X}^N$, $y^N \in \mathcal{Y}^N$, and $W, \hat{W} \in \{1, \dots, 2^{NR}\}$.

measure. The existence of a good lossy source coding codebook for any $R > C$ is proved by a random coding argument, i.e., by showing that the average error probability over the randomly chosen ensemble of codebooks is small.

Finally, the equivalence between \mathcal{N} of capacity C and \mathcal{C} of rate R can be established when $R = C$ based on the continuity of the capacity region. Readers are referred to [1] for a rigorous and thorough treatment.

Note that the jointly typical pairs (x^N, y^N) that are used to construct the channel emulation codebooks are taken from a “restricted” typical set $\hat{A}_\epsilon^{(N)}$ where the associated decoding error probability (assuming x^N is transmitted through the original noisy channel) is smaller than a threshold. Sequences that do not satisfy this condition are expurgated. That is, given the classical typical set

$$T_\epsilon^{(N)} = \{(x^N, y^N) \mid \left| \frac{1}{N} \log(p(x^N, y^N)) - H(X, Y) \right| < \epsilon\},$$

the restricted typical set is defined [1] as

$$\hat{A}_\epsilon^{(N)} = \{(x^N, y^N) \mid (x^N, y^N) \in T_\epsilon^{(N)}, p(T_\epsilon^{(N)} | x^N) > \frac{1}{2}\}.$$

The concept of capacity upper and lower bounding models developed in [1] has been extended to independent multi-terminal channels in [2] following similar arguments as illustrated in Fig. 1, and multiplicative and additive gaps between lower and upper bounding models for independent multi-terminal channels have been established. Illustrative upper and lower bounding models for MACs/BCs/ICs involving two transmitters and/or two receivers have been demonstrated in [2]–[4]. Given a noisy network composed by independent building blocks whose upper and lower bounding models are available, we can replace these building blocks with their corresponding upper (resp. lower) bounding models and then characterize an outer (resp. inner) bound for its capacity region based on the resulting noiseless network models.

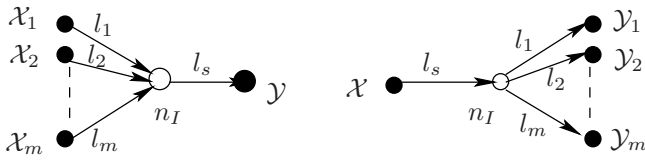


Fig. 2. The one-shot upper bounding models for MACs/BCs with m transmitters/receivers. The white nodes indicated by n_I are auxiliary operation nodes to specify the rate constraints on the sum rate and on individual rates. All the channels are noiseless bit pipes and independent from others. The one-shot upper bounding models are fully characterized by the rate vector $(R_{l_s}, R_{l_1}, \dots, R_{l_m})$, where R_{l_i} is the rate of the noiseless bit pipe l_i .

For wireless networks, however, it may be difficult in general to apply directly the channel emulation technique to construct bounding models, as the coupled components may involve many transmitting/receiving nodes. For coupled single-hop networks which can be modeled as ICs, the bounding models are difficult to characterize even for the simplest 2×2 setup [2]. For coupled multi-hop non-layered networks, it is unclear how the channel emulation technique can be extended to incorporate the interaction among different transmitting-receiving pairs across different layers. Although one may apply the cut-set bound [10] to construct upper bounds for wireless networks, the resulting analysis may become quite involved, as illustrated in [29]–[32], for characterizing upper bounds for small size relay networks. Moreover, even if we manage to construct bounding models for a specific coupled network, we have to create new bounding models for each different network topology, which makes it unscalable for wireless networks that have diversified communication scenarios and topologies.

C. One-shot Bounding Models

Instead of using emulation with channel coding or lossy source coding to construct bounding models as in [1], [2], a class of one-shot upper bounding models have been proposed in [6] for independent MACs/BCs, where an auxiliary operation node is introduced for each MAC/BC to facilitate separate characterization of the sum rate and the individual rates. As illustrated in Fig. 2, all the channels in the one-shot upper bounding models are point-to-point bit pipes which can be fully characterized by the rate vector $(R_{l_s}, R_{l_1}, \dots, R_{l_m})$, where R_{l_i} is the rate of the bit pipe l_i . The rate constraint R_{l_i} can either be constructed by channel emulation over the stacked network as in [1], [2], or by channel emulation that is realized in each instance corresponding to a channel use (hence referred to as “one-shot” approach). For example, we can construct the sum rate constraint by stacked emulation whilst bound individual rates by one-shot emulation, or the other way around, which results in two types of upper bounding models [6]. To highlight the specific channel emulation method used on each link, we illustrate in Fig. 3 the explicit operation of the auxiliary node by specifying its input/output alphabets.

1) *One-Shot Channel Emulation for Individual Rate Constraints*: For MACs with m transmitters, say $\mathcal{N}_{MAC} = (\prod_{i=1}^m \mathcal{X}_i, p(y|\mathbf{x}), \mathcal{Y})$, the one-shot emulation for the channel from transmitter with alphabet \mathcal{X}_i sends exactly the corresponding source symbol $X_i \in \mathcal{X}_i$ to the auxiliary operation

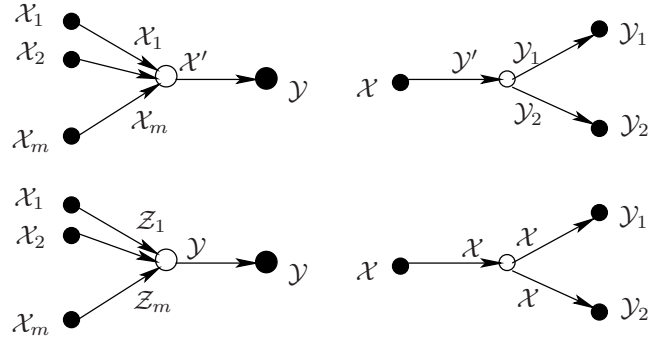


Fig. 3. Illustration of the two types one-shot upper bounding models [6] for m -user MACs and for two-user BCs: $\mathcal{C}_{u,MAC,1}$ (upper left), $\mathcal{C}_{u,MAC,2}$ (lower left), $\mathcal{C}_{u,BC,1}$ (upper right), and $\mathcal{C}_{u,BC,2}$ (lower right). The operation of the auxiliary operation nodes are explicitly specified by the associating input/output alphabets, where $\mathcal{X}' = \prod_{i=1}^m \mathcal{X}_i$ and $\mathcal{Y}' = \mathcal{Y}_1 \times \mathcal{Y}_2$ are compound input/output alphabets, and $Z_i \in \mathcal{Z}_i, i = 1, \dots, m$ are auxiliary random variables to synthesize $Y \in \mathcal{Y}$ through a predefined function $y = g(z_1, \dots, z_m)$ as described in (15).

node n_I , hence requiring a noiseless bit pipe of rate $R_{l_i} \geq \log(|\mathcal{X}_i|)$. The auxiliary node then combines all the inputs together and formulates a super alphabet $\mathcal{X}' = \prod_{i=1}^m \mathcal{X}_i$. The channel from n_I to the receiver is then simply a point-to-point channel with input alphabet \mathcal{X}' and output alphabet \mathcal{Y} . This setup is illustrated in Fig. 3 (upper left). By the network equivalence theory for point-to-point channels [1], successful channel emulation requires

$$R_{l_s} \geq R_{MAC} \triangleq \max_{p(\mathbf{x}')} I(\mathcal{X}'; Y) = \max_{p(x_1, \dots, x_m)} I(X_1, \dots, X_m; Y). \quad (9)$$

Hence, we can construct the upper bounding model as

$$\mathcal{C}_{u,MAC,1} = (R_{MAC}, \log(|\mathcal{X}_1|), \dots, \log(|\mathcal{X}_m|)). \quad (10)$$

Similarly, for a BC with two receivers $\mathcal{N}_{BC} = (\mathcal{X}, p(y_1, y_2|x), \mathcal{Y}_1 \times \mathcal{Y}_2)$, the channel from the source to the auxiliary operation node n_I has a super output alphabet $\mathcal{Y}' = \mathcal{Y}_1 \times \mathcal{Y}_2$, which results in a sum rate constraint

$$R_{BC} \triangleq \max_{p(x)} I(X; \mathcal{Y}') = \max_{p(x)} I(X; Y_1, Y_2). \quad (11)$$

After successfully receiving $Y' = [Y_1, Y_2]$, the auxiliary node n_I sends exactly the corresponding symbol Y_i to the receiver with alphabet \mathcal{Y}_i , hence requiring a noiseless bit pipe of rate $R_{l_i} \geq \log(|\mathcal{Y}_i|)$. This setup is illustrated in Fig. 3 (upper right). The corresponding upper bounding model is therefore

$$\mathcal{C}_{u,BC,1} = (R_{BC}, \log(|\mathcal{Y}_1|), \log(|\mathcal{Y}_2|)). \quad (12)$$

2) *One-Shot Channel Emulation for Sum Rate Constraint*: Alternatively, one may bound the sum rate by one-shot channel emulation and then specify individual rates. For the two-user BC \mathcal{N}_{BC} , the one-shot emulation sends every X from the source to the auxiliary node, which requires a sum rate constraint of $\log(|\mathcal{X}|)$. Then the auxiliary node sends X to the two receivers through independent channels, each requires a rate constraint

$$R_i \triangleq \max_{p(x)} I(X; Y_i), i = 1, 2. \quad (13)$$

This setup is illustrated in Fig. 3 (lower right) and the corresponding upper bounding model is

$$\mathcal{C}_{u,BC,2} = (\log(|\mathcal{X}|), R_1, R_2), \quad (14)$$

which is valid only if the noise at two receivers are independent, i.e., the transition probability can be factorized as

$$p(y_1, y_2|x) = p(y_1|x)p(y_2|x).$$

For the m -user MAC \mathcal{N}_{MAC} , the setup for channel emulation is illustrated in Fig. 3 (lower left) where $z_i \in \mathcal{Z}_i$ is an auxiliary random variable for the channel from \mathcal{X}_i such that [6]

$$p(y|x_1, \dots, x_m) = \sum_{\substack{z_1, \dots, z_m: \\ y=g(z_1, \dots, z_m)}} \prod_{i=1}^m p(z_i|x_i), \quad (15)$$

where $g: \prod_i \mathcal{Z}_i \rightarrow \mathcal{Y}$ is a predefined deterministic function

$$y = g(z_1, z_2, \dots, z_m), \quad (16)$$

to reproduce the channel output Y at the auxiliary node n_I . From stacked channel emulation we can get the individual rate constraints as follows

$$R_i \triangleq \max_{p(x_i)} I(X_i; Z_i), i = 1, \dots, m. \quad (17)$$

Therefore the corresponding one-shot model can be written as

$$\mathcal{C}_{u,MAC,2} = (\log(|\mathcal{Y}|), R_1, \dots, R_m). \quad (18)$$

Here we give two examples to show how to construct the auxiliary random variables as specified by (15). For Gaussian MACs, auxiliary random variables can be constructed based on a noise partitioning approach, i.e., the additive noise at the destination is partitioned into independent parts and allocated to each of the individual channels. For a two-user Gaussian MAC with noise power $\sigma^2=1$ and the received power constraint γ_i for X_i , the corresponding upper bounding model is

$$\mathcal{C}_{u,MAC,2} = \left(\log(|\mathcal{Y}|), \frac{1}{2} \log \left(1 + \frac{\gamma_1}{\alpha} \right), \frac{1}{2} \log \left(1 + \frac{\gamma_2}{1-\alpha} \right) \right), \quad (19)$$

where $\alpha \in (0, 1)$ is the noise partitioning parameter chosen to minimize the total input rate

$$R_s = \frac{1}{2} \log \left(1 + \frac{\gamma_1}{\alpha} \right) + \frac{1}{2} \log \left(1 + \frac{\gamma_2}{1-\alpha} \right). \quad (20)$$

For binary additive MAC $\{0, 1\}^2 \rightarrow \{0, 1\}$ with Bernoulli distortion $Bern(\epsilon)$, the corresponding distortion parameter ϵ_i for channel l_i should satisfy

$$\epsilon = \epsilon_1(1 - \epsilon_2) + \epsilon_2(1 - \epsilon_1). \quad (21)$$

Remark 1: Although $\mathcal{C}_{u,MAC,1}$ and $\mathcal{C}_{u,BC,1}$ are tight on sum rate in the sense that there are some kind of networks where the sum rate constraint R_{MAC} (R_{BC}) is tight, the constraints on individual rates are somewhat loose. $\mathcal{C}_{u,MAC,2}$ and $\mathcal{C}_{u,BC,2}$, on the other hand, have tighter bounds on individual rates but looser on sum rate.

3) *Gap in One-shot Bounding Models:* The gap between the upper and lower bounding models for Gaussian channels and for binary symmetric channels have been examined in [6], where a gap less than 1/2 bit per channel use has been established for MACs with two transmitters and BCs with two receivers.

III. BOUNDING MODELS FOR NON-COUPLED NETWORKS

For non-coupled networks, which can be decomposed into independent MACs/BCs and point-to-point channels, we first construct upper and lower bounding models for MACs/BCs, which can then be used to substitute their noisy counterparts in construction of noiseless bounding models for the original noisy network. To give a full description of all the rate constraints on any subset of transmitters/receivers, the upper and lower bounding models for independent MACs/BCs with m transmitters/receivers need to consist of $(2^m - 1)$ rate constraints. However, such an approach is not scalable as m can be quite large in many practical scenarios. Instead, we introduce a rate vector of length up to $(m+1)$ to specify our upper and lower bounding models.

For independent MACs/BCs with m transmitters/receivers, our upper bounding models inherit the one-shot model structure as illustrated in Fig. 2 and therefore only contain constraints on each of the maximum allowed individual rate R_i , $i = 1, \dots, m$, and the total sum rate. All the constraints on subsets of individual rates, i.e.,

$$R(S) \triangleq \sum_{i \in S} R_i, S \subset \{1, \dots, m\}, \text{ and } 2 \leq |S| < m, \quad (22)$$

are omitted, which results in a looser but simpler upper bound. The benefits of keeping the one-shot structure are two fold: they can be extended to MACs/BCs with m transmitters/receivers at low complexity; they facilitate our proposed channel decoupling method in a natural way for constructing the upper and lower bounding bounds for coupled networks.

A. Upper Bounding Models for Independent MACs with m Transmitters

For MACs with m transmitters, the one-shot bounding model $\mathcal{C}_{u,MAC,1}$ defined in (10) focuses solely on the sum rate and $\mathcal{C}_{u,MAC,2}$ defined in (18) focuses solely on individual rates. To facilitate a tradeoff between the sum rate constraint and each of the individual rate constraints, we propose here a new upper bounding model,

$$\begin{aligned} \mathcal{C}_{u,MAC,new} &= (R_s, R_1, \dots, R_m), \quad (23) \\ R_s &= \max_{p(v_1, \dots, v_m)} I(V_1 \dots V_m; Y), \\ R_i &= \max_{p(x_i)} I(X_i; V_i), i = 1, \dots, m, \end{aligned}$$

where V_1, \dots, V_m are auxiliary random variables introduced to account for the noise ‘‘allocation’’ to each individual rate constraint through V_i and its conditional probability $p(v_i|x_i)$ such that

$$p(v_1, \dots, v_m|x_1, \dots, x_m) = \prod_{i=1}^m p(v_i|x_i). \quad (24)$$

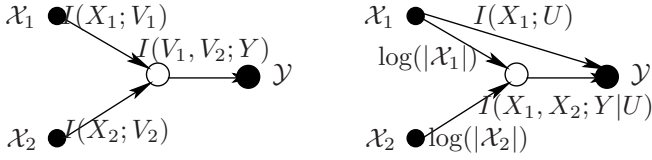


Fig. 4. Upper bounding models for independent MACs with two transmitters: the new bounding model $\mathcal{C}_{u,MAC,new}(\alpha)$ (left) and the model developed in [2, Theorem 6] with $p(u, y|x_1, x_2) = p(u|x_1)p(y|x_1, x_2)$ (right). The label on each bit pipe is the minimum rate requirement for any given $p(x_1, x_2)$.

Noise allocation to the sum rate constrain is through V_1, \dots, V_m and the conditional probability $p(y|v_{[1:m]})$ such that

$$p(y, v_1, \dots, v_m|x_1, \dots, x_m) = p(y|v_{[1:m]})p(v_{[1:m]}|x_{[1:m]}), \quad (25)$$

i.e., $Y - V_{[1:m]} - X_{[1:m]}$ forms a Markov chain.

For the new upper bounding model $\mathcal{C}_{u,MAC,new}$, we introduce a parameter $\alpha \in [0, 1]$ to quantify the proportion of noise distortion that has been “allocated” to the sum rate constraint R_s . It is determined by the type of the channel/noise via its channel transition function $p(y|x_{[1:m]})$ and by the auxiliary random variables V_1, \dots, V_m via the conditional probability function $p(y|v_{[1:m]})$. When all the noise distortion is put into R_s , i.e., $V_i = X_i, \forall i$ and thus $p(y|v_{[1:m]}) = p(y|x_{[1:m]})$, we have $\alpha=1$ and the corresponding sum rate constraint R_s is the tightest. When no noise is put into R_s , i.e., when Y is fully determined by V_1, \dots, V_m and thus $H(Y|V_1 \dots V_m) = 0$, we have $\alpha=0$ and the sum rate constraint is relaxed to the one-shot upper bound $\log(|\mathcal{Y}|)$. The explicit dependence of $\alpha \in [0, 1]$ and the noise allocation is determined by the type of the noise. For example, for additive noise with average power constraint, we may use the proportion of noise power to evaluate α . Another option is to define α as the ration between $H(Y|V_1 \dots V_m)$ and $H(Y|X_1 \dots X_m)$, provided that the latter is finite.

Remark 2: The parameterized bounding model $\mathcal{C}_{u,MAC,new}$ includes the two one-shot models as special cases: putting all distortion into R_s ($\alpha=1$) will generate $\mathcal{C}_{u,MAC,1}$, which give us a tighter bound R_{MAC} on the sum rate but looser constraints on all individual rates; taking no noise into R_s ($\alpha=0$) will produce $\mathcal{C}_{u,MAC,2}$, which leads to looser bound on the sum rate but tighter bounds on individual rates.

1) *2-user MACs:* For 2-user MACs, it is interesting to compare the new upper bounding model $\mathcal{C}_{u,MAC,new}$ with the model developed in [2, Theorem 6], as illustrated in Fig. 4. On one hand, setting $V_1=X_1$ and $V_2=X_2$ will put all the distortion components into the sum rate constraint (i.e., $\alpha = 1$), which results in an upper bounding model

$$\mathcal{C}_{u,MAC,new}(\alpha=1) = (\max_{p(x_1, x_2)} I(X_1, X_2; Y), \log(|\mathcal{X}_1|), \log(|\mathcal{X}_2|)). \quad (26)$$

It is the same as the upper bounding model in [2, Theorem 6] when $U=\emptyset$. On the other hand, if we choose $V_1=U$ and a deterministic function $f: \mathcal{U} \times \mathcal{V}_2 \rightarrow \mathcal{Y}$ such that $y=f(u, v_2)$

and $p(u, v_2|x_1, x_2)=p(u|x_1)p(v_2|x_2)$, we can generate another bounding model

$$\mathcal{C}_{u,MAC,new}(\alpha=0) = (\log(|\mathcal{Y}|), \max_{p(x_1)} I(X_1; U), \max_{p(x_2)} I(X_2; V_2)). \quad (27)$$

Compared to the bound in [2, Theorem 6], it is clear that $\mathcal{C}_{u,MAC,new}(\alpha=0)$ has a tighter bound on rate R_1 . However, as we will show below, $\mathcal{C}_{u,MAC,new}(\alpha=0)$ has a looser bound on rate R_2 .

Lemma 1: Given $p(u, v_2|x_1, x_2)=p(u|x_1)p(v_2|x_2)$ and $y=f(u, v_2)$, we have

$$I(X_1, X_2; Y|U) \leq \min\{I(X_2; V_2), \log(|\mathcal{X}_2|), \log(|\mathcal{Y}|)\}. \quad (28)$$

Proof:

$$\begin{aligned} I(X_1, X_2; Y|U) &= H(Y|U) - H(Y|X_1, X_2, U) \\ &= H(V_2|U) - H(V_2|X_2) \\ &\leq H(V_2) - H(V_2|X_2) \\ &= I(X_2; V_2) \leq \log(|\mathcal{X}_2|), \end{aligned} \quad (29)$$

where the second equality is due to $y=f(u, v_2)$ and the fact that $U - (X_1, X_2) - V_2$ and $X_1 - X_2 - V_2$ are Markov chains, and the first inequality comes from the fact that condition reduces entropy, with equality if and only if X_1, X_2 (and thus U, V_2) are independent. On the other hand, we can also rewrite (29) as

$$\begin{aligned} 0 \leq I(X_1, X_2; Y|U) &\leq H(Y) - H(Y|X_1, X_2, U) \\ &= I(Y; X_1, X_2, U) \leq \log(|\mathcal{Y}|). \end{aligned} \quad (30)$$

Combining (29) and (30), we have (28). \blacksquare

Furthermore, if we are only interested in a tight bound on sum rate, by Lemma 2 below, we can see that choosing a non-trivial auxiliary random variable U in [2, Theorem 6] can not improve the sum rate constraint.

Lemma 2: Given $p(u, x_1, x_2, y) = p(u|x_1)p(x_1, x_2)p(y|x_1, x_2)$, we have

$$I(X_1; U) + I(X_1, X_2; Y|U) \geq I(X_1, X_2; Y), \quad (31)$$

with equality if and only if $I(X_1, X_2; U|Y) = 0$.

Proof:

$$\begin{aligned} I(X_1, X_2; Y|U) &= I(X_1, X_2; Y) + I(X_1, X_2; U|Y) - I(X_1, X_2; U) \\ &= I(X_1, X_2; Y) + I(X_1, X_2; U|Y) - I(X_1; U) - I(X_2; U|X_1) \\ &= I(X_1, X_2; Y) + I(X_1, X_2; U|Y) - I(X_1; U) \\ &\geq I(X_1, X_2; Y) - I(X_1; U), \end{aligned}$$

where the first two equalities are due to the chain rule, the third equality comes from the Markov chain $U - X_1 - X_2$ (thus $I(X_2; U|X_1) = 0$), and the last in equality comes from the fact that mutual information is non-negative, with equality if and only if $I(X_1, X_2; U|Y) = 0$. \blacksquare

2) *m*-user Gaussian MAC: Given noise power $\sigma^2=1$ and the received power constraint γ_i for $X_i, i=1, \dots, m$, the sum rate is upper bounded by

$$R_{MAC} = \frac{1}{2} \log \left(1 + \left(\sum_{i=1}^m \sqrt{\gamma_i} \right)^2 \right), \quad (32)$$

which can be achieved only if all the transmitters can fully cooperate.

The parameterized new upper bounding model $\mathcal{C}_{u,MAC,new}(\alpha)$ defined in (23) can be constructed as follows. Let $Z_i, i = 0, \dots, m$, be independent Gaussian random variable with zeros mean and variance $\alpha_i > 0$ such that $\alpha_0 = \alpha$ and $\sum_{i=0}^m \alpha_i = 1$. By choosing the auxiliary random variables $V_i = X_i + Z_i, i = 1, \dots, m$, we have

$$Y = V_1 + \dots + V_m + Z_0, \quad (33)$$

and all the rate constraints in $\mathcal{C}_{u,MAC,new}(\alpha)$ can be written as

$$R_s(\alpha) = \frac{1}{2} \log \left(1 + \frac{(\sum_{i=1}^m \sqrt{\gamma_i})^2 + 1 - \alpha}{\alpha} \right), \quad (34)$$

$$R_i(\alpha) = \frac{1}{2} \log \left(1 + \frac{\gamma_i}{\alpha_i} \right), \quad i = 1, \dots, m. \quad (35)$$

Remark 3: If we are interested in a tighter bound on any individual rate, say on R_{li} , we can partition the noise by setting $\alpha = 0$ and $\alpha_i = 1$, which leads to a tighter constraint $R_i = \frac{1}{2} \log(1 + \gamma_i)$ on rate R_{li} but unbounded constraints on all other individual rates and the sum rate. If we are only interested in a tighter bound on the sum rate, setting $\alpha = 1$ will give us a tight bound R_{MAC} on the sum rate but unbounded constraints on all individual rates.

For given $\alpha \in [0, 1)$, one way to determine the noise partitioning parameters $\alpha_i, i = 1, \dots, m$ is to solve the following optimization problem

$$\begin{aligned} \min_{\alpha_1, \dots, \alpha_m} \quad & \sum_{i=1}^m \log \left(1 + \frac{\gamma_i}{\alpha_i} \right), \\ \text{subject to} \quad & \sum_{i=1}^m \alpha_i = 1 - \alpha, \\ & \alpha_i > 0. \end{aligned} \quad (36)$$

This is a convex optimization problem whose solution can be explicitly found by Lagrangian methods [33] as follows (see Appendix A for details),

$$\alpha_i^* = \frac{\sqrt{\gamma_i(\gamma_i + 4\mu)} - \gamma_i}{2}, \quad i = 1, \dots, m,$$

where μ satisfies

$$\frac{1}{2} \sum_{i=1}^m \left(\sqrt{\gamma_i(\gamma_i + 4\mu)} - \gamma_i \right) = 1 - \alpha. \quad (37)$$

Although solving this problem in closed-form is challenging, as the specific value of μ depends both on α and the relative magnitude of all γ_i , its upper and lower bounds can be determined as shown by Lemma 3 below. Since the LHS of (37) is monotonously increasing with respect to μ , it is

simple to find μ numerically by evaluating (37) within the region defined by Lemma 3.

Lemma 3: Given $\alpha \in [0, 1]$ and $\gamma_i > 0, i = 1, \dots, m$, the μ defined by (37) is bounded by

$$\frac{1 - \alpha}{m} + \frac{(1 - \alpha)^2}{m} \frac{1}{\sum_i \gamma_i} \leq \mu \leq \frac{1 - \alpha}{m} + \frac{(1 - \alpha)^2}{m^2} \frac{1}{\min_i \gamma_i}, \quad (38)$$

where both equalities hold if and only if $\gamma_1 = \dots = \gamma_m$.

Proof: See Appendix B. ■

From Lemma 4 below, we can see that the freedom of adjusting $\alpha \in [0, 1]$ in the optimized noise partition (36) can not improve the sum rate constraint R_{MAC} . This is intuitive as R_{MAC} is achievable when all the source nodes can fully cooperate.

Lemma 4: Given $\gamma_1, \dots, \gamma_m > 0$, for any $\alpha \in [0, 1]$, we have

$$\min \{ R_s(\alpha), \sum_{i=1}^m R_i(\alpha) \} \geq R_{MAC}, \quad (39)$$

with equality when $\alpha = 1$.

Proof: See Appendix C. ■

B. Upper Bounding Models for Independent BCs with *m* Receivers

The upper bounding model for independent BCs with *m* receivers can be generalized straightforwardly from [6] as follows

$$\mathcal{C}_{u,BC,1} = (R_{BC}, \log(|\mathcal{Y}_1|), \dots, \log(|\mathcal{Y}_m|)), \quad (40)$$

$$\mathcal{C}_{u,BC,2} = (\log(|\mathcal{X}|), R_1, \dots, R_m), \quad (41)$$

where

$$R_{BC} \triangleq \max_{p(x)} I(X; Y_1, \dots, Y_m), \quad (42)$$

$$R_i \triangleq \max_{p(x)} I(X; Y_i), \quad i = 1, \dots, m. \quad (43)$$

Note that $\mathcal{C}_{u,BC,1}$ is a valid upper bound for any channel transition function $p(y_1, \dots, y_m|x)$ whereas $\mathcal{C}_{u,BC,2}$ is only valid for BC with independent noise components at receivers, i.e., when the transition probability can be factorized as

$$p(y_1, \dots, y_m|x) = \prod_{i=1}^m p(y_i|x).$$

1) *New Upper Bounding Models for m-user BCs:* We construct a new upper bounding model by combining the point-to-point channel emulation technique developed in [1] with the *Covering Lemma*, *Conditional Typicality Lemma*, and the *Joint Typicality Lemma* [34]. Let $[l_1, l_2, \dots, l_m]$ denote a permutation of the *m* receivers and $[Y_1, Y_2, \dots, Y_m]$ be their corresponding channel outputs, whose dependence is characterized by the channel transition function $p(y_1, \dots, y_m|x)$. The new bounding model is represented by

$$\mathcal{C}_{u,BC,new} = (R_s, R_{l_1}, R_{l_2}, \dots, R_{l_m}), \quad (44)$$

$$R_{l_k} = \max_{p(x)} I(X; Y_1, \dots, Y_k), \quad k=1, \dots, m,$$

$$R_s = R_{l_m} = \max_{p(x)} I(X; Y_1, \dots, Y_m),$$

where R_s is the sum rate constraint from the transmitter to the auxiliary node n_I , and R_{l_k} is the rate constraint from n_I to receiver l_k .

Remark 4: Compared to the upper bounding model $\mathcal{C}_{u,BC,1}$ specified in (40), the new model $\mathcal{C}_{u,BC,new}$ maintains the tight sum rate constraint R_{BC} as specified in (42) and meanwhile improves all the individual rate constraints.

Below we show step-by-step how to construct the new bounding model given in (44). To simplify notation, for $k=1, \dots, m$, let $Y_{[1:k]}$ represent the sequence of k random variables $\{Y_1, Y_2, \dots, Y_k\}$ and $w_{[1:k]}$ be the sequence of k integers (w_1, w_2, \dots, w_k) . The channel emulation is done over a stacked network with N replicas of the original BC.

Step I: Fix a channel input distribution $p_X(x)$. As defined in [1], let $\hat{A}_\epsilon^{(N)}(X)$ be a subset of the classical typical⁵ set $T_\epsilon^{(N)}(X)$ [34] such that for any $x^N \in \hat{A}_\epsilon^{(N)}(X)$ as the input to the BC, the probability that the corresponding output sequences $\{y_1^N, y_2^N, \dots, y_m^N\}$ are not jointly typical with x^N is smaller than a predefined threshold. Furthermore, let $p_{Y_{[1:k]}}(y_1, \dots, y_k)$, $k=1, \dots, m$, be marginal distributions obtained from $p(x, y_1, \dots, y_m) = p(y_1, \dots, y_m|x)p_X(x)$, and define a series of conditional distributions as follows

$$p(y_{k+1}|y_{[1:k]}) \triangleq \begin{cases} 0, & \text{if } p_{Y_{[1:k]}}(y_{[1:k]}) = 0, \\ \frac{p_{Y_{[1:k+1]}}(y_{[1:k+1]})}{p_{Y_{[1:k]}}(y_{[1:k]})}, & \text{otherwise.} \end{cases} \quad (45)$$

Step II: Generate independently at random $2^{NR'_1}$ sequences $\{y_1^N(w_1) : w_1=1, \dots, 2^{NR'_1}\}$, each according to $\prod_i p_{Y_i}(y_{1,i})$. For any sequence $x^N \in \hat{A}_\epsilon^{(N)}(X)$, by the *Covering Lemma* [34],

$$\lim_{N \rightarrow \infty} Pr \left(\exists w_1 \in [1 : 2^{NR'_1}], \text{ s.t. } (x^N, y_1^N(w_1)) \in T_{\epsilon_1}^{(N)} \right) = 1, \quad (46)$$

if $R'_1 > I(X; Y_1) + \delta_1(\epsilon_1)$ for some $\epsilon_1 > \epsilon > 0$ and $\delta_1(\epsilon_1) > 0$ that goes to zero as $\epsilon_1 \rightarrow 0$. Following the channel emulation argument [1], we define a mapping function $\alpha_1(x^N)$ as

$$\alpha_1(x^N) = \begin{cases} w_1, & \text{if } \exists w_1 \text{ s.t. } (x^N, y_1^N(w_1)) \in T_{\epsilon_1}^{(N)}, \\ 1, & \text{otherwise.} \end{cases} \quad (47)$$

If more than one sequence are jointly typical with x^N , $\alpha_1(x^N)$ chooses one of them uniformly at random.

Step III: For each sequence $y_1^N(w_1)$, generate independently $2^{NR'_2}$ sequences $\{y_2^N(w_1, w_2) : w_2=1, \dots, 2^{NR'_2}\}$, each according to $\prod_i p(y_{2,i}|y_{1,i}(w_1))$, where $p(y_2|y_1)$ is defined in (45). Given $w_1 = \alpha_1(x^N)$, according to the *Conditional Typicality Lemma* [34], we have

$$Pr \left((x^N, y_1^N(w_1)) \in T_{\epsilon_1}^{(N)}(XY_1) \right) \rightarrow 1 \text{ as } N \rightarrow \infty, \quad (48)$$

and according to the *Joint Typicality Lemma* [34], for all $w_2 \in [1 : 2^{NR'_2}]$,

$$Pr \left((x^N, y_1^N(w_1), y_2^N(w_1, w_2)) \in T_{\epsilon_2}^{(N)}(XY_1Y_2) \right) \geq 2^{-N(I(X; Y_2|Y_1) + \delta_2(\epsilon_2))}, \quad (49)$$

⁵In this subsection, the typical set $T_\epsilon^{(N)}$ is defined based on the strong typicality to support the *Conditional Typicality Lemma* and the *Joint Typicality Lemma*.

for $\epsilon_2 > \epsilon_1$ and some $\delta_2(\epsilon_2) > 0$ that goes to zeros as $\epsilon_2 \rightarrow 0$. Since sequences $\{y_2^N(w_1, \cdot)\}$ are i.i.d given w_1 , we have

$$\begin{aligned} & Pr \left(\forall w_2 \in [1 : 2^{NR'_2}], (x^N, y_1^N(w_1), y_2^N(w_1, w_2)) \notin T_{\epsilon_2}^{(N)} \right) \\ &= \left(Pr \left((x^N, y_1^N(w_1), y_2^N(w_1, w_2)) \notin T_{\epsilon_2}^{(N)} \right) \right)^{2^{NR'_2}} \\ &\leq \left(1 - 2^{-N(I(X; Y_2|Y_1) + \delta_2(\epsilon_2))} \right)^{2^{NR'_2}} \\ &\leq exp \left(-2^{NR'_2} \cdot 2^{-N(I(X; Y_2|Y_1) + \delta_2(\epsilon_2))} \right) \\ &= exp \left(-2^{N(R'_2 - I(X; Y_2|Y_1) - \delta_2(\epsilon_2))} \right), \end{aligned} \quad (50)$$

where the first inequality comes from (49) and the second inequality comes from the fact that $(1-x)^n \leq exp(-nx)$, $\forall x \in [0, 1]$. Therefore if $R'_2 > I(X; Y_2|Y_1) + \delta_2(\epsilon_2)$, the probability that none of the sequences in $\{y_2^N(w_1, w_2) : w_2 \in [1 : 2^{NR'_2}]\}$ is joint typical with $(x^N, y_1^N(w_1))$ tends to 0 as $N \rightarrow \infty$. We now define a mapping function $\alpha_2(x^N, w_1)$ as follows

$$\alpha_2(x^N, w_1) = \begin{cases} w_2, & \text{if } (x^N, y_1^N(w_1), y_2^N(w_1, w_2)) \in T_{\epsilon_2}^{(N)}, \\ 1, & \text{otherwise.} \end{cases} \quad (51)$$

If there is more than one candidate that satisfies the joint typicality condition, $\alpha_2(\cdot)$ chooses one of them uniformly at random.

Step IV: For $k = 3, \dots, m$, we treat the set of sequences $\{y_1^N(w_1), \dots, y_{k-1}^N(w_{[1:k-1]})\}$ together as one unit and repeat Step III, which generates the corresponding sequences $\{y_k^N(w_{[1:k-1]}, w_k) : w_k=1, \dots, 2^{NR'_k}\}$, the mapping function $\alpha_k(x^N, w_{[1:k-1]})$, and the rate constraint

$$R'_k > I(X; Y_k|Y_{[1:k-1]}) + \delta_k(\epsilon_k), \quad (52)$$

where $\epsilon_k > \epsilon_{k-1}$, and $\delta_k(\epsilon_k) > 0$ that goes to zeros as $\epsilon_k \rightarrow 0$.

Step V: Define a channel emulation codebook

$$\{y_k^N(w_1, \dots, w_k) : k=1, \dots, m, w_k=1, \dots, 2^{R'_k}\}, \quad (53)$$

and the associated encoding function $\alpha(x^N) = [\alpha_1(\cdot), \dots, \alpha_m(\cdot)]$ and the decoding function $\alpha_k^{-1}(w_{[1:k]})$ for receiver l_k , $k=1, \dots, m$. For any input x^N , $\alpha(x^N)$ generates a sequence (w_1, w_2, \dots, w_m) of $N \sum_{i=1}^m R'_i$ bits that are transmitted from the transmitter of the BC to the auxiliary node n_I , which then forwards them to receiver l_k . At receiver l_k , the decoding function $\alpha_k^{-1}(w_{[1:k]})$ selects a sequence from the codebook $\{y_k^N\}$ based on the received information bits, i.e.,

$$\alpha_k^{-1}(w_1, \dots, w_k) = y_k^N(w_1, \dots, w_k).$$

Note that the rate constraints in (52) should be satisfied for $k=1, \dots, m$, and for all $p_X(x)$. Let $N \rightarrow \infty$ and $\epsilon_m \rightarrow 0^6$, we can specify all the rate constraints in (44) as follows

$$R_{l_k} = \sum_{i=1}^k R'_i = \max_{p(x)} I(X; Y_1, \dots, Y_k), \quad k=1, \dots, m, \quad (54)$$

$$R_s = R_{l_m} = \max_{p(x)} I(X; Y_1, \dots, Y_m). \quad (55)$$

⁶Since $0 < \epsilon < \epsilon_1 < \dots < \epsilon_m$, letting $\epsilon_m \rightarrow 0$ implies that all of them go to zero.

The second equality in (54) comes from the fact that

$$I(X; Y_{[1:k]}) = I(X; Y_1) + I(X; Y_2|Y_1) + \dots + I(X; Y_k|Y_{[1:k-1]}), \quad (56)$$

and the first equality in (55) comes from our emulator design as specified in Step V.

Remark 5: There are in total $m!$ different permutations of l_1, \dots, l_m , each leading to a different upper bounding model following our construction method. For each of these upper bounding models, the sum rate constraint and one of the individual rate constraints are tight. Depending on the needs, we can select a specific permutation to design the upper bounding model.

Remark 6: For BC with $m = 2$ receivers, the proposed upper bounding model has two different layouts $\mathcal{C}_{u,BC,a} = (R_{BC}, R_1, R_{BC})$ and $\mathcal{C}_{u,BC,b} = (R_{BC}, R_{BC}, R_2)$, where the latter turns out to be equivalent to the upper bounding model developed in [2, Theorem 5]. This is not surprising as the channel emulation codebook $\{y_1^N, y_2^N\}$ used in our construction is generated in the same way as in [2, Theorem 5]: superposition encoding. Note that the proof in [2, Theorem 5], restricted for BC with $m=2$ receivers, provides explicit error analysis. In contrast, our construction is valid for $m \geq 2$ but only claims that the error probability can be made arbitrarily small with the help of the *Covering Lemma*, the *Conditional Typicality Lemma*, and the *Joint Typicality Lemma*.

2) Extension to m -user BCs with Continuous Alphabets:

The error analysis in our construction of new upper bounding models for m -user BCs in Sec. III-B1 relies on the validity of the *Covering Lemma*, the *Conditional Typicality Lemma*, and the *Joint Typicality Lemma*, which hold for discrete-alphabet channels under strong/robust typicality notions. There are several possible approaches to extend our results in Sec. III-B1 to continuous alphabets.

One way is to apply the standard discretization procedure [34, Chp. 3.4.1] to continuous alphabets⁷ and then apply the results derived based on discrete alphabets. Such process has been demonstrated in [34, Chp. 3.4.1] to prove the achievability of AWGN channel capacity, and in [15] to extend separation results from DMC to AWGN channels with a per-symbol average power constraint.

Another way is to use generalized typicality definitions such that the *Covering Lemma* (which essentially depends on the *Conditional Typicality Lemma*) and the *Joint Typicality Lemma* can be extended to continuous alphabets. For example, joint typicality properties associated with strong typicality have been extended to countably infinite alphabets in [35] by a notion of unified typicality. The *Generalized Markov Lemma* has been extended in [36] to Gaussian sources with a modified notion of typicality and by the fact that the asymptotic equipartition property (AEP) holds for Gaussian memoryless sources. Other attempts in this direction can be found, for example, in [37] where the *covering lemma* and *packing lemma* are extended to continuous alphabets (memoryless source) and in [38] where the likelihood encoder [39] with the soft-covering

⁷As described in [34, Chp. 3.4.1], the transition function of the continuous-alphabet channel should be “well-behaved” to facilitate the discretization and quantization procedure.

TABLE I
ALL POSSIBLE RATE CONSTRAINTS IN THE LOWER BOUNDING MODEL
FOR BROADCAST CHANNELS WITH m RECEIVERS.

$R_i, i =$	1	2	3	...	$2^m - 1$
$i : \{0, 1\}^m$	0...001	0...010	0...011	...	1...111
$\{\mathcal{D}_n\}, n =$	1	2	2, 1	...	$m, \dots, 2, 1$

lemma [39], [40] is applied to the lossy source compression with continuous alphabets.

We may also construct our new upper bounding models in Sec. III-B1 by iteratively applying the method developed in [2, Theorem 5]: We first only focus on two channel outputs Y_1, Y_2 , and construct a valid upper bound for this 2-user BC $\mathcal{X} \rightarrow \mathcal{Y}_1 \times \mathcal{Y}_2$ as in [2, Theorem 5]; then we treat $[Y_1, Y_2] \in \mathcal{Y}_1 \times \mathcal{Y}_2$ as a single compound receiver and group it with Y_3 to formulate a new 2-user BC, whose upper bound can also be constructed as in [2, Theorem 5]; we can repeat this process until there is no more receivers to be included. However, the associated error analysis can be very involved.

C. Lower Bounding Models for Independent MACs and BCs

Our lower bounding models for MACs/BCs are constructed directly based on some operating points within the achievable rate region assuming no transmitter/receiver cooperation. However, the structure of the lower bounding models are quite different for MACs and BCs. The main difference between MACs and BCs is the encoding process. When there is no transmitter/receiver cooperation, distributed encoding is performed in MACs while centralized encoding is done in BCs. As a consequence, in MAC setups, only one rate constraint is needed for each point-to-point bit pipe to fully describe any operation point within the rate region. In BCs, each of the private messages dedicated for one specific receiver may also be decoded by other receivers. Such “overheard” messages (the common messages) should be reflected in the rate region, which requires the usage of point-to-points bit pipes (hyper-arc) in the lower bounding model.

1) *MACs with m Transmitters:* The lower bounding models can be constructed by choosing an operating point in the capacity region of the MAC assuming independent sources. We can choose any point in the capacity region that can be achieved by using independent codebooks at transmitters and successive interference cancellation decoding at the receiver. For Gaussian MAC with m transmitters, each with received SNR $\gamma_i, i = 1, \dots, m$, the following sum rate is achievable

$$R_{l,s} = \frac{1}{2} \log \left(1 + \sum_{i=1}^m \gamma_i \right). \quad (57)$$

2) *BCs with m Receivers:* For BCs, each of the private messages dedicated for one specific receiver may also be decoded by other receivers, and such overheard messages can be useful when the BCs are part of a larger network. To model such message overhearing, we need to introduce point-to-points bit pipes (i.e., hyper-arcs) to represent multicast rate constraints. For BCs with m receivers $\{\mathcal{D}_n, n = 1, \dots, m\}$, there are in total $(2^m - 1)$ subsets of receivers, each corresponding to a unique rate constraint. As illustrated in Table I, we denote

R_i as the rate constraint corresponding to successful decoding at receivers indicated by the locations of ‘1’ in the length- m binary expression of the index i . For example, R_3 is the constraint for the multicast rate to receivers \mathcal{D}_2 and \mathcal{D}_1 , and R_{2^m-1} is the constraint for multicast rate to all receivers. Depending on the channel quality, we represent the lower bounding mode by a vector⁸ \mathbf{R} which contains one sum rate constraint (denoted by R_0) and up to m constraints⁹ from Table I. We illustrate this by an example of Gaussian BCs with m receivers.

Example: Gaussian BCs with m Receivers Let γ_i be the received SNR at receiver \mathcal{D}_i , $i = 1, \dots, m$. Without loss of generality, assuming $\gamma_1 \leq \gamma_2 \leq \dots \leq \gamma_m$, we divided the total information into m distinct messages $\{W_i, i = 1, \dots, m\}$. By superposition coding of W_i with power allocation parameters $\beta_i \in [0, 1]$, $\sum_{i=1}^m \beta_i = 1$, at the transmitter, and successive interference cancellation at each receiver¹⁰, successful decoding of W_i can be realized at a set of receivers $\{\mathcal{D}_n, n = i, \dots, m\}$ with multicast/unicast rate

$$R_{2^m-2^{i-1}} = \frac{1}{2} \log \left(1 + \frac{\beta_i \gamma_i}{1 + \gamma_i \sum_{j=i+1}^m \beta_j} \right). \quad (58)$$

For example, successful decoding of W_1 can be realized at all receivers with a multicast rate of R_{2^m-1} , and successful decoding of W_m can only be realized at receiver \mathcal{D}_m with a unicast rate of R_{2^m-1} . The resulting rate vector is therefore

$$\mathbf{R} = [R_0, R_{2^m-2^{i-1}} : i = 1, \dots, m], \quad (59)$$

where the sum-rate constraint R_0 is

$$R_0 = \sum_{i=1}^m R_{2^m-2^{i-1}} = \sum_{i=1}^m \frac{1}{2} \log \left(\frac{1 + \gamma_i \sum_{j=i}^m \beta_j}{1 + \gamma_i \sum_{j=i+1}^m \beta_j} \right) \quad (60)$$

$$= \frac{1}{2} \log(1 + \gamma_1) + \frac{1}{2} \sum_{i=2}^m \log \left(\frac{1 + \gamma_i \sum_{j=i}^m \beta_j}{1 + \gamma_{i-1} \sum_{j=i}^m \beta_j} \right). \quad (61)$$

The last equality comes from the fact that

$$\sum_{i=1}^m \beta_i = 1.$$

Since $\gamma_{i-1} \leq \gamma_i$, the function $\frac{1+x\gamma_i}{1+x\gamma_{i-1}}$ is monotonically increasing on $x \in [0, 1]$, with its maximum $\frac{1+\gamma_i}{1+\gamma_{i-1}}$ achieved when $x = 1$. It is simple to show that

$$R_0 \leq \frac{1}{2} \log(1 + \gamma_m), \quad (62)$$

where the equality is achieved when $\beta_m = 1$ (i.e., $\beta_i = 0$ for all $i \neq m$).

Remark 7: Note that power allocation at the transmitter of a BC allows elimination of weakest receivers. For example,

⁸For each R_i in \mathbf{R} we also need to store its index i to specify the receiving subset.

⁹For statistically degraded m -receiver BCs (e.g., Gaussian BCs), m constraints are sufficient by creating a physically degraded channel via proper coding schemes, and the rate loss will vanish in low SNR regime [5]. For non-degraded channels, we only focus on the first m most significant non-zero constraints.

¹⁰Alternatively, one can encode W_1 to W_m successively by dirty paper coding [41] and use a maximum likelihood decoder at each receiver.

by setting $\beta_1 = \beta_2 = 0$ in (58) the weakest two receivers \mathcal{D}_1 and \mathcal{D}_2 will have nothing to decode and hence be removed from the set of destinations.

D. Gaps between Upper and Lower Bounding Models for Gaussian MACs and BCs

For Gaussian MACs with m transmitters, the sum rate is upper bounded by R_{MAC} given by (32), and lower bounded by $R_{l,s}$ given by (57). The gap between the upper and the lower bounds on sum rate, measured in bits per channel use, is therefore bounded by

$$\begin{aligned} \Delta_{MAC} &= R_{MAC} - R_{l,s} = \frac{1}{2} \log \left(\frac{1 + (\sum_{i=1}^m \sqrt{\gamma_i})^2}{1 + \sum_{i=1}^m \gamma_i} \right) \\ &\leq \frac{1}{2} \log \left(\frac{1 + m \sum_{i=1}^m \gamma_i}{1 + \sum_{i=1}^m \gamma_i} \right) < \frac{1}{2} \log(m), \end{aligned} \quad (63)$$

where the first inequality comes from Jensen’s inequality based on the convexity of the function $f(x) = x^2$. Hence, for Gaussian MACs with transmitters in isolation, feedback and transmitter cooperation can increase the sum capacity by at most $\frac{1}{2} \log(m)$ bits per channel use.

For Gaussian BCs with m receivers, the sum rate is lower bounded by R_0 given by (62) and upper bounded by

$$R_{BC} = \frac{1}{2} \log \left(1 + \sum_{i=1}^m \gamma_i \right). \quad (64)$$

Note that R_{BC} can be achieved only when full cooperation among all receivers is possible. The gap between the upper and the lower bounds on the sum rate is therefore

$$\begin{aligned} \Delta_{BC} &= R_{BC} - R_0 = \frac{1}{2} \log \left(\frac{1 + \sum_{i=1}^m \gamma_i}{1 + \gamma_m} \right) \\ &\leq \frac{1}{2} \log \left(\frac{1 + m\gamma_m}{1 + \gamma_m} \right) < \frac{1}{2} \log(m), \end{aligned} \quad (65)$$

where the first inequality comes from the assumption $\gamma_i \leq \gamma_m$ for all i . Hence, for m -receiver Gaussian BCs with all receivers in isolation, feedback and receiver cooperation can increase the sum capacity by at most $\frac{1}{2} \log(m)$ bits per channel use.

The gap between upper and lower bounding models becomes considerably smaller at low SNR or when the SNR for each link diverges. For example, with $\gamma_1 = 1, \gamma_2 = 2, \gamma_3 = 100$ (e.g., 0, 3, 20dB, respectively), the gaps (measured in bits per channel use) are

$$\begin{aligned} \Delta_{MAC} &= \frac{1}{2} \log \left(\frac{1 + (1 + \sqrt{2} + 10)^2}{1 + 1 + 2 + 100} \right) \approx 0.29, \\ \Delta_{BC} &= \frac{1}{2} \log \left(\frac{1 + 1 + 2 + 100}{1 + 100} \right) \approx 0.02, \end{aligned}$$

which are much smaller than $\frac{1}{2} \log(3) \approx 0.79$.

IV. BOUNDING MODELS FOR COUPLED NETWORKS

Capacity bounding models for MACs and BCs developed in [2]–[4], [6] and extensions presented in Sec. III are all designed for networks with non-coupled MACs/BCs. In wireless networks, however, a signal dedicated for one receiver may also be overheard by its neighbors, owing to the broadcast

nature of wireless transmission. A transmit signal can be designed for multiple destinations (as in BCs) and the received signal may consist of signals from several source nodes (as in MACs) and thus interfere with each other. Although such dependence among coupled BCs and MACs has been partially treated in [2] by grouping coupled transmitter-receiver pairs together as ICs, whose bounding models require up to $m(2^m - 1)$ bit pipes for IC with m transmitter-receiver pairs, the whole family of multi-hop non-layered channels (e.g., relay channels) remains untreated.

Inspired by the idea of separate sum and individual rate constraints [6], we choose to incorporate dependent transmitter-receiver pairs into coupled BCs and MACs. With the help of a new channel decoupling method introduced below, we can decompose a coupled sub-network into decoupled BCs and MACs. The noisy channel that connects a pair of decoupled BC and MAC is split into two parts by channel decoupling, and their dependence will be taken into account when constructing bounding models for the BC and the MAC.

A. Channel Decoupling

Given a memoryless network

$$\mathcal{N}_T = \left(\prod_v \prod_i \mathcal{X}_{v,i}, p(\mathbf{y}|\mathbf{x}), \prod_v \prod_j \mathcal{Y}_{v,j} \right),$$

where $\mathcal{X}_{v,i}$ is the input alphabet of the i -th outgoing channel and $\mathcal{Y}_{v,j}$ is the output alphabet of the j -th incoming channel associated with node v , all the channel input-output dependence can be fully characterized by the transition function $p(\mathbf{y}|\mathbf{x})$. Based on the dependence of input/output alphabets, we rewrite the transition function into product format and partition the network \mathcal{N}_T into *independent* point-to-point channels \mathcal{N}_i , MACs $\mathcal{N}_{S_j \rightarrow j}$, BCs $\mathcal{N}_{k \rightarrow D_k}$, and sub-networks $\mathcal{N}_{S_l \rightarrow D_l}$. A sub-network $\mathcal{N}_{S_l \rightarrow D_l}$ can be further decomposed into independent channels and smaller sub-networks as long as there exist non-trivial complementary subsets (S, S^c) of S_l and (D, D^c) of D_l such that

$$p(\mathbf{y}_{D_l}|\mathbf{x}_{S_l}) = p(\mathbf{y}_D|\mathbf{x}_S)p(\mathbf{y}_{D^c}|\mathbf{x}_{S^c}). \quad (66)$$

We repeat this partition process until we can't decompose the sub-networks any further.

To highlight all independent components within the network, we rewrite the network expression as

$$\mathcal{N}_T = \prod_i \mathcal{N}_i \times \prod_j \mathcal{N}_{S_j \rightarrow j} \times \prod_k \mathcal{N}_{k \rightarrow D_k} \times \prod_l \mathcal{N}_{S_l \rightarrow D_l}, \quad (67)$$

where \prod and \times indicate channel independence as defined in Definition 1. To construct capacity bounding models for \mathcal{N}_T , we replace each independent point-to-point channel by a bit pipe with rate equal its channel capacity as prescribed by [1]. For all the independent MACs and BCs, we replace them by their corresponding upper and lower bounding models developed in Sec. III. The independent sub-networks need some special treatment as we will discuss below.

For an independent sub-network $\mathcal{N} = \left(\prod_{l=1}^n \mathcal{X}_l, p(\mathbf{y}|\mathbf{x}), \prod_{k=1}^m \mathcal{Y}_k \right)$ that contains n transmitting

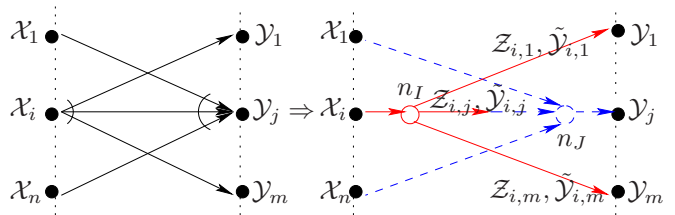


Fig. 5. An independent sub-network $\mathcal{N} = \left(\prod_{l=1}^n \mathcal{X}_l, p(\mathbf{y}|\mathbf{x}), \prod_{k=1}^m \mathcal{Y}_k \right)$ in which a BC with input alphabet \mathcal{X}_i and a MAC with output alphabet \mathcal{Y}_j are coupled by the noisy connection $\mathcal{X}_i \rightarrow \mathcal{Y}_j$. After channel decoupling, the decoupled MAC is characterized by $p(y_j|\mathbf{x})$ given in (68), and the decoupled BC is characterized by $p(z_i|x_i)$ given in (73) for upper bounding models and by $\tilde{p}_L(\tilde{y}_i|x_i)$ given in (72) for lower bounding models. The auxiliary random variables $Z_{i,j}$ are introduced for upper bounding models and $\tilde{Y}_{i,j}$ for lower bounding models.

alphabets and m receiving alphabets, as shown in the left part of Fig. 5, the BC with input alphabet \mathcal{X}_i and the MAC with output alphabet \mathcal{Y}_j are coupled due to the noisy connection $\mathcal{X}_i \rightarrow \mathcal{Y}_j$. Note that $p(\mathbf{y}|\mathbf{x})$ does not necessarily indicate a layered structure of the sub-network; rather it is only an abstraction of the input-output dependence of the network (cf. the relay channel with $p(y, y_r|x, x_r)$). Our channel decoupling approach that will be presented in Sec. IV-A1 has two essential components: the auxiliary node with its associated input/output alphabets, and the new probability functions designed to describe the decoupled MACs and BCs. When constructing bounding models for the decoupled MACs and BCs, there will be two individual rate constraints on the bit pipe corresponding to the connection $\mathcal{X}_i \rightarrow \mathcal{Y}_j$: one from the decoupled BC with input alphabet \mathcal{X}_i and one from the decoupled MAC with output alphabet \mathcal{Y}_j . Since both of the two constraints are introduced to characterize the same individual rate, they should be simultaneously respected when constructing the noiseless bounding models. We demonstrate this principle in Sec. IV-B for the upper bounding models and in Sec. IV-C for the lower bounding models.

1) *Transition Functions for Decoupled MACs/BCs:* As mentioned in Sec. I, in this paper we assume that the distortion components in a noisy coupled network are mutually independent, i.e., the transition probability can be partitioned as

$$p(\mathbf{y}|\mathbf{x}) = \prod_{j=1}^m p(y_j|\mathbf{x}),$$

where

$$p(y_j|\mathbf{x}) \triangleq \sum_{\mathbf{y}_j} p(\mathbf{y}|\mathbf{x}), \quad (68)$$

is the marginal distribution for Y_j given \mathbf{X} . We characterize the decoupled MAC with received alphabet \mathcal{Y}_j by the marginal distribution $p(y_j|\mathbf{x})$, which preserves the possibility of source cooperation (allowing all possible $p(\mathbf{x})$ as in \mathcal{N}). We can then construct its upper and lower bounding models based on $p(y_j|\mathbf{x})$ by following the techniques developed in Sec. III-A and in Sec. III-C1, respectively. However, the lower bounding models will be updated in Sec. IV-C to incorporate potential interference.

Note that by treating each of the decoupled MACs individually, the resulting capacity upper bound for the sub-network can be looser than the bound when we treat the sub-network without decomposition. For any given $p(\mathbf{x})$, we have

$$I(\mathbf{X}; \mathbf{Y}) = h(\mathbf{Y}) - h(\mathbf{Y}|\mathbf{X}) = h(\mathbf{Y}) - \sum_{j=1}^m h(Y_j|\mathbf{X}) \quad (69)$$

$$\leq \sum_{j=1}^m h(Y_j) - h(Y_j|\mathbf{X}) = \sum_{j=1}^m I(\mathbf{X}; Y_j), \quad (70)$$

where the inequality is due to the correlation among \mathbf{Y} . This is intuitive as we can always treat \mathbf{X} as a compound source and the sub-network as a virtual BC: treating each output channel as an independent channel will result in looser rate constraints. However, as we have discussed earlier, the bounding models for multiple-input multiple-output sub-networks are difficult to obtain even for the simplest 2×2 setup, and there is no systematic approach for constructing upper and lower bounding models as the size of the sub-network grows.

The decoupled BC with transmit alphabet \mathcal{X}_i can't be fully described by its marginal

$$p(\mathbf{y}|x_i) \triangleq \sum_{\mathbf{x}_{/i}} p(\mathbf{y}|\mathbf{x})p(\mathbf{x}_{/i}|x_i), \quad (71)$$

since $p(\mathbf{y}|x_i)$ is determined not only by $p(\mathbf{y}|\mathbf{x})$ itself, but also by all the possible distributions of channel inputs $\mathbf{X}_{/i}$. Therefore $p(\mathbf{y}|x_i)$ only provides a description of the average behavior of the correlation among different channel outputs but erases both the explicit dependence of \mathbf{Y} on a specific channel input and the interaction among different channel inputs \mathbf{X} .

To preserve the structure of the original coupled network and to capture the input-output dependence in the decoupled BCs, we define a transition function with transmit alphabet \mathcal{X}_i as

$$\tilde{p}_L(\tilde{\mathbf{y}}_i|x_i) \triangleq p(\mathbf{y}|x_i, \mathbf{x}_{/i} = \emptyset), \quad (72)$$

where $\mathbf{x}_{/i} = \emptyset$ represents the scenario that there is no input signal¹¹ except $X_i = x_i$, and $\tilde{\mathbf{Y}}_i$ are auxiliary random variables introduced to represent the corresponding channel output. The transition function defined in (72) will be first used to construct **lower bounding models** for the decoupled BC using the techniques developed in Sec. III-C2, where a specific coding scheme (e.g., superposition with rate and power allocation) is designed for X_i . The effect of interference from other signals will be incorporated into the lower bounding models in the two-step update presented in Sec. IV-C. Note that the definition (72) accommodates the explicit dependence of channel outputs on the input signal $X_i = x_i$ but erases source cooperation. It therefore enables efficient and simple characterization of the individual and sum rate constraints (optimized over $p(x_i)$) which are otherwise difficult to obtain (optimized over $p(\mathbf{x})$). Furthermore, it preserves possible noise correlation in \mathbf{Y} which will be useful in future work.

¹¹For additive channels this implies that we force $\mathbf{x}_{/i} = 0$ even if $0 \notin \mathcal{X}_j$, $j \neq i$. For multiplicative channels, we set $\mathbf{x}_{/i} = 1$.

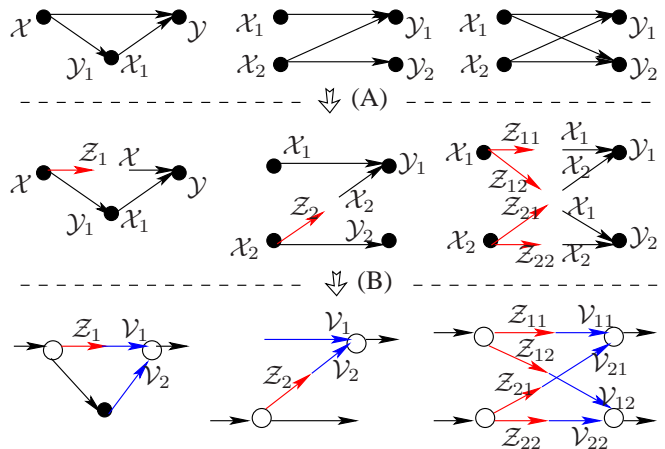


Fig. 6. Illustration of channel decoupling (A) and upper bounding process (B) for the relay channel, the two-user Z-channel, and the two-user X-channel. After channel decoupling, the output of the decoupled BCs are changed from \mathcal{Y} to \mathcal{Z} (highlighted in red) as described by (73) and input to the decoupled MACs inherent the original alphabets as described by (68). To construct upper bounding models for each decoupled two-user MAC, we introduced two auxiliary random variables (highlighted in blue) as described by (23)–(24) in Sec. III-A.

To construct **upper bounding models** for decoupled BCs, we introduce a group of auxiliary random variables

$$\begin{aligned} \mathbf{Z} &\triangleq \{Z_{i,j}|i=1, \dots, n, j=1, \dots, m\} \\ &= \{Z_i|i=1, \dots, n\} = \{Z^j|j=1, \dots, m\}, \end{aligned}$$

and a predefined function $\mathbf{Y} = g(\mathbf{Z})$ such that

$$p(\mathbf{y}|\mathbf{x}) = \sum_{\mathbf{z}: \mathbf{y}=g(\mathbf{z})} \prod_{i=1}^n p(\mathbf{z}_i|x_i), \quad (73)$$

where $\mathbf{z}_i = [z_{i,1}, \dots, z_{i,m}]$ is the corresponding “output” vector of the input signal $X_i = x_i$ and $\mathbf{z}^j = [z_{1,j}, \dots, z_{n,j}]$ is the decomposed output vector from received signal $Y_j = y_j$. The corresponding upper bounding models for the decoupled BC with transition probability $p(\mathbf{z}_i|x_i)$ can be therefore constructed following the techniques developed in Sec. III-B. However, as in the case for decoupled MACs, treating each decoupled BC individually in constructing upper bounding models will result in a looser capacity upper bound than treat them all together (if possible). For any given $p(\mathbf{x})$, we have

$$I(\mathbf{X}; \mathbf{Y}) \leq I(\mathbf{X}; \mathbf{Z}_1, \dots, \mathbf{Z}_n) \quad (74)$$

$$= h(\mathbf{Z}_1, \dots, \mathbf{Z}_n) - h(\mathbf{Z}_1, \dots, \mathbf{Z}_n|\mathbf{X}) \quad (75)$$

$$= h(\mathbf{Z}_1, \dots, \mathbf{Z}_n) - \sum_i h(\mathbf{Z}_i|\mathbf{X}_i) \quad (76)$$

$$\leq \sum_i h(\mathbf{Z}_i) - \sum_i h(\mathbf{Z}_i|\mathbf{X}_i) \quad (77)$$

$$= \sum_i I(X_i; \mathbf{Z}_i), \quad (78)$$

where (74) is due to $\mathbf{Y} = g(\mathbf{Z})$, (76) comes from (73) and the fact that $X_j - X_i - Z_i$ forms a Markov chain for all $i \neq j$, and (77) is due to chain rule and the fact that condition reduces entropy.

In Fig. 6 we illustrate the operation of channel decoupling for the three-node relay channel, the two-user Z-channel, and

the two-user X-channel. Note that we do not specify the transmission task (e.g., unicast or multicast) for the Z-channel and the X-channel since our bounding models are designed for general transmission schemes rather than tailored/optimized for any specific communication task. For the relay channel, the decoupled MAC is the same as if the source-relay link were not present, and the decoupled BC has an auxiliary random variable Z_1 that depends on X but not X_1 , but meanwhile must reflect the distortion component at the destination when constructing upper bounding models. A different auxiliary random variable \tilde{Y}_1 will be introduced here when constructing lower bounding models as described by (72). It is clear that choosing Z_1 and \tilde{Y}_1 such that $X-Z_1-\tilde{Y}_1$ formulates a Markov chain can satisfy all the previous constraint. The decoupling operation for the Z-channel is similar. The X-channel is decoupled into two MACs and two BCs, and for each decoupled BC we introduce auxiliary random variables $Z_{i,j}$ and $\tilde{Y}_{i,j}$ for constructing upper and lower bounding models, respectively.

2) *Channel Decoupling via Noise Partition for Gaussian Networks*: For Gaussian coupled networks, the auxiliary variables $\mathbf{Z} = \{Z_{i,j} | i=1, \dots, n, j=1, \dots, m\}$ can be determined by the noise partition approach as in Sec. III-A. Let $\mathbf{H} = [h_{i,j}]_{n \times m}$ be the matrix of channel coefficients such that

$$\mathbf{y} = \mathbf{H}^T \mathbf{x} + \mathbf{w} = [h_1, \dots, h_n] \mathbf{x} + \mathbf{w}, \quad (79)$$

where \mathbf{h}_i is the column vector of channel coefficients from source node i to all receiving nodes, \mathbf{x} is the transmitting vector with average power constraint $E[|x_i|^2] \leq P_i$, and \mathbf{w} is the vector of noise with zero mean and unit variance. We can partition the noise components into independent terms such that

$$\mathbf{z}_i = \mathbf{h}_i x_i + \mathbf{w}_i, \quad (80)$$

where $\mathbf{w}_i = [w_{i,1}, \dots, w_{i,m}]^T$ is the vector of partitioned noise components w.r.t. the input signal x_i and the variance of $w_{i,j}$ is denoted by $\alpha_{i,j} > 0$. Define $\gamma_{i,j} = P_i * |h_{i,j}|^2$, the noise partition parameters $\alpha_{i,j}$ (and hence $z_{i,j}$) can be determined by the following optimization problem

$$\begin{aligned} \min_{\alpha_{i,j}} \quad & \sum_{i=1}^n \log \left(1 + \sum_{j=1}^m \frac{\gamma_{i,j}}{\alpha_{i,j}} \right), \\ \text{subject to} \quad & \sum_{i=1}^n \alpha_{i,j} = 1, \quad \forall j \in \{1, \dots, m\}, \\ & \alpha_{i,j} > 0. \end{aligned} \quad (81)$$

Note that (81) is a convex optimization problem whose solution can be explicitly found by Lagrangian methods [33] as shown in Appendix D.

B. Upper Bounding Models

Given a memoryless coupled noisy network with independent noise, we first apply the channel decoupling method proposed in Sec. IV-A to decompose it into decoupled MACs and BCs. The upper bounding models for the decoupled BC with transmit alphabet \mathcal{X}_i can be constructed by techniques developed in Sec. III-B, with the transition probability $p(\mathbf{z}_i | x_i)$

given in (73), where the auxiliary random variables $Z_{i,j}$ that depends only on X_i is introduced by a noise partition approach. The upper bounding models for the decoupled MAC with receive alphabet \mathcal{Y}_j are constructed based on the transition function $p(y_j | \mathbf{x})$ given in (68), and auxiliary random variables $V_{i,j}$ that also only depend on X_i are introduced by (23)–(24) in Sec. III-A to reflect the “contribution” from input signal X_i to the output signal Y_j . We illustrated this upper bounding process in Fig. 6 for the relay channel, the two-user Z-channel, and the two-user X-channel. Note that the auxiliary random variables $Z_{i,j}$ defined in (73) and $V_{i,j}$ defined in (23)–(24), though introduced on different stages, depend only on the same X_i and are given by the same “noise partition” approach. We can therefore introduce them in such a way that either $X_i - Z_{i,j} - V_{i,j}$ or $X_i - V_{i,j} - Z_{i,j}$ can formulate a Markov chain. Then, for each pair of decoupled BC and MAC, the corresponding bit pipe that connects them in the upper bounding model should take the rate constraint that equals the maximum of the two required rates (one from each side).

In the channel decomposition and upper bounding model construction, we have introduced some auxiliary random variables based on the “noise partition” approach. Although our approach cannot be applied to **all channels**, it does apply to at least two types of channels: additive channels with additive noise, e.g., $Y_j = Z_j + \sum_i H_{ij} X_i$, and multiplicative channels with multiplicative noise, e.g., $Y_j = Z_j \cdot \prod_i H_{ij} X_i$. The former has been demonstrated via the Gaussian networks in (19) and (80), and the latter has been illustrated via the two-user binary additive MAC in (21) where the channel can be represented as a binary multiplicative channel $Y = X_1 X_2 Z$ with alphabets $\{\pm 1\}$. Even though these two channel types cannot be used to represent all channels, they cover the vast majority of channel models used in publications on wireless communication and networks.

According to the max-flow min-cut theorem, the maximum throughput from source to sink can be no larger than the value of the minimum cut in between. For each transmission task (unicast or multiple cast), we identify all the cuts in the resulting upper bounding network (which contains only noiseless point-to-point connections) and calculate the flows across each cut. The resulting capacity region is therefore an outer bound¹² for the upper bounding network, and hence also an outer bound for the original coupled noisy network.

C. Lower Bounding Models

The MACs/BCs lower bounding models presented in Sec. III-C, see also [2]–[4], [6], are designed for independent MACs and BCs, rather than handling the possible interaction among transmitted/received signals by neighboring nodes in a coupled network. Although such interaction has been considered in [2] for constructing the lower bounding models for

¹²As shown in [18], the max-flow min-cut theorem is tight on some noiseless networks, which include noiseless networks associated with single-source multiple-unicast transmission, single-source (two-level) multicast transmission, and multi-source multicast transmission. Therefore the bound we obtained by the max-flow min-cut theorem might be the capacity region for the corresponding upper bounding network.

2×2 ICs, and in [28] to approximate the capacity of multiple unicast transmission over bidirectional wireless channels with symmetric fading coefficients, scalable lower bounding models for general transmission tasks over wireless networks are still not available.

After channel decoupling, the decoupled MAC with receive alphabet \mathcal{Y}_j is described by $p(y_j|\mathbf{x})$ given in (68), and the decoupled BC with transmit alphabet \mathcal{X}_i is characterized by the transition probability $\tilde{p}_L(\tilde{\mathbf{y}}_i|x_i)$ defined in (72). Since the transmit signals x_i from the decoupled BC may contain messages that are not designed for decoding at the decoupled MAC, we have to incorporate such interfering signals into account through a two-step update as presented in Sec. IV-C1. The two-step update is based on the intrinsic feature of successive interference cancellation decoding, where the message currently under decoding suffers interference from non-decoded messages. We start from BCs where a specific coding scheme (e.g., superposition coding with rate splitting and power allocation) is designed for transmitting signal X_i based on $\tilde{p}_L(\tilde{\mathbf{y}}_i|x_i)$, and then we go to the decoupled MACs where a specific successive decoding order is determined based on $p(y_j|\mathbf{x})$ and the encoding strategies that sending \mathbf{x} . Once the decoding order is fixed, we know exactly how much interference one message will suffer from other messages and we can modify the corresponding rate on each bit pipe.

Below we show step-by-step how to construct lower bounding models for decoupled MACs/BCs with a two-step update in Sec. IV-C1 and demonstrate it via a coupled Gaussian network in Sec. IV-C2.

1) Step-by-Step Construction:

Step I: Network Decomposition

Apply the channel decoupling method proposed in Sec. IV-A to decompose the coupled sub-networks into decoupled BCs and MACs.

Step II: Lower Bounding Models for Point-to-Point Channels, BCs, and Independent MACs

We replace each independent point-to-point channel with a bit pipe whose rate equals its capacity [1]. For each BC and each independent MAC, we replace them with the corresponding lower bounding models as described in Sec. III-C2 and in Sec. III-C1, respectively. Note that in this step the lower bounding models for decoupled BCs are constructed assuming no interference.

Step III: Lower Bounding Models for Decoupled MACs

A decoupled MAC has one or more input signals originated from decoupled BCs. When constructing lower bounding models in Step II, a specific encoding scheme is adopted by each of the decoupled BCs, whose message might not be fully decoded at the decoupled MAC. From the encoding schemes of decoupled BCs, we can identify the signal components that can't be decoded by the decoupled MAC (hence behave as interference). With such information about the interfering signals, we can construct lower bounding models for the decoupled MAC by integrating the interference effect into the models developed in Sec. III-C1.

Step IV: Rate Adjustment for Decoupled BCs

The lower bounding models for a decoupled MAC has prescribed a specific decoding strategy, e.g., in which order

the messages are decoded. During the successive decoding process, messages decoded in earlier stages experience higher level of interference. The lower bounding models for the decoupled BCs should be updated to reflect the exact amount of interference encountered during the decoding process. Such update is crucial to ensure that the broadcasting messages from the decoupled BC can be successfully decoded by all intended receivers.

After **Step IV** we have generate a lower bounding network consists of only noiseless bit pipes, including point-to-points bit pipes (i.e., hyper-arcs) that carry the same data from one point to multiple points. The problem of finding the optimal scheme to manage the data flows over such noiseless networks is in general open. However, there exist many heuristic (and thus suboptimal in general) methods, see [42] for example, for constructing a valid inner bound.

2) *Example: Lower Bounding Models for a Coupled Gaussian $m \times n$ Network:* We illustrate the lower bounding process for a coupled Gaussian network $\mathcal{N} = (\prod_{i=1}^m \mathcal{X}_i, p(\mathbf{y}|\mathbf{x}), \prod_{j=1}^n \mathcal{Y}_j)$, where for all feasible (i, j) , the channel from X_i to Y_j has SNR γ_{ij} (incorporating the transmitted signal power and the corresponding channel gain). We first decompose the coupled network into decoupled MACs and BCs. For illustration purpose, we only focus on a pair of decoupled MAC and BC that share a common channel $\mathcal{X}_i \rightarrow \mathcal{Y}_j$. Let $\mathcal{N}_{i \rightarrow D_i} = (\mathcal{X}_i, p(y_{D_i}|x_i), \prod_{k \in D_i} \mathcal{Y}_k)$ be the decoupled BC with transmit signal X_i and $\mathcal{N}_{S_j \rightarrow j} = (\prod_{k \in S_j} \mathcal{X}_k, p(y_j|\mathbf{x}_{S_j}), \mathcal{Y}_j)$ be the decoupled MAC with receive signal Y_j . Without loss of generality, we assume that $D_i \subset \{1, \dots, n\}$, $S_j \subset \{1, \dots, m\}$ such that $i \in S_j$, $j \in D_i$, $|S_j| \geq 2$ and $|D_i| \geq 2$.

As in **Step II**, we first construct lower bounding models for the decoupled BC $\mathcal{N}_{i \rightarrow D_i}$ based on the rate and power allocation strategy as described in Sec. III-C2. Depending on the channel quality, the messages carried by X_i may contain components that are not intended for decoding at the decoupled MAC $\mathcal{N}_{S_j \rightarrow j}$. The component(s) of X_i that can't be decoded by $\mathcal{N}_{S_j \rightarrow j}$ will therefore behave as interference during the decoding process. We denote the power of the interfering component from X_i at Y_j by Γ_{ij} , and the exact value can be obtained from the lower bounding model of $\mathcal{N}_{i \rightarrow D_i}$. We have $\Gamma_{ij} = 0$ if all messages contained in X_i are intended for successful decoding, and $\Gamma_{ij} = \gamma_{ij}$ if nothing is to be decoded. After careful examination of all input signals \mathbf{x}_{S_j} , the total power of interfering components contained in Y_j is given by

$$P_j^I = \sum_{k \in S_j} \Gamma_{kj}. \quad (82)$$

We can now construct the lower bounding model for the decoupled MAC $\mathcal{N}_{S_j \rightarrow j}$ in **Step III** based on the effective SNR, which is defined as

$$\hat{\gamma}_{kj} = \frac{\gamma_{kj} - \Gamma_{kj}}{1 + P_j^I}, \quad \forall k \in S_j. \quad (83)$$

For $k \in S_j$, let l_k indicate the order of successive decoding in constructing the MAC lower bounding model: $l_i = 1$ means X_i is the first to be decoded. When decoding the message

conveyed by signal X_i , the amount of interference introduced by signals other than X_i is

$$P_{i,j}^I = \sum_{\substack{k \in S_j \\ l_k < l_i}} \Gamma_{kj} + \sum_{\substack{k \in S_j \\ l_k < l_i}} \gamma_{kj}. \quad (84)$$

We call $P_{i,j}^I$ the “extrinsic interference” of X_i suffered during the decoding process of Y_j .

After Step III, we have obtained by (84) the extrinsic interference power $P_{i,k}^I$ caused by input signals other than X_i in the decoupled MAC with output signal Y_k , for all $k \in D_i$. As suggested in **Step IV**, we should now update the lower bounding models for decoupled BC $\mathcal{N}_{i \rightarrow D_i}$ constructed in Step II by taking these extrinsic interference into account. To facilitate straightforward comparison with the lower bounding models developed in Sec. III-C2, without loss of generality¹³, we assume $D_i = \{1, \dots, n\}$ with $\gamma_{i1} \leq \dots \leq \gamma_{in}$.

The rate constraint $R_{2^n - 2^{l-1}}$ defined by (58) in Sec. III-C2, which corresponds to the multicast rate to a subset of receivers associated with $\{Y_k : k = l, l+1, \dots, n\}$, should be adjusted by taking into account the extrinsic interference power $\{P_{i,k}^I : k = l, l+1, \dots, n\}$. The corresponding new rate constraint, denoted by $R'_{2^n - 2^{l-1}}$, is therefore defined as

$$R'_{2^n - 2^{l-1}} = \min_{k \in \{l, l+1, \dots, n\}} \frac{1}{2} \log \left(1 + \frac{\gamma_{ik} \beta_l}{1 + P_{i,k}^I + \gamma_{ik} \sum_{t=l+1}^n \beta_t} \right). \quad (85)$$

The sum-rate constraint should be adjusted accordingly, i.e.,

$$R'_0 = \sum_{l=1}^n R'_{2^n - 2^{l-1}}. \quad (86)$$

Note that the minimum operation in (85) comes from the fact that given $\gamma_{il} \leq \dots \leq \gamma_{in}$, we can't guarantee

$$\frac{\gamma_{il}}{1 + P_{i,l}^I} \leq \dots \leq \frac{\gamma_{in}}{1 + P_{i,n}^I} \quad (87)$$

due to the effect of the extrinsic interference caused by decoupled MACs. Here we simply keep the structure of the original lower bounding model unchanged without claiming its optimality.

Although we only demonstrate the two-step update via a Gaussian example, this approach is also feasible for non-Gaussian additive noise. For point-to-point channel, Gaussian noise is the most pessimistic given the same SNR constraint. For decoding at MACs, Gaussian noise is also the most pessimistic since we can always treat all the received signals as if they were sent from a single transmitter via superposition encoding with power allocation.

Remark 8: In our approach the effect of interference due to non-decoded messages has been incorporated in the two-step update process where successive interference cancellation decoding is used at all receiving nodes. Alternatively, one may treat the $m \times n$ coupled network together and design a feasible coding approach with better interference management. For example, in [28] an inner bound for the capacity region of a

coupled bidirectional network with ergodic symmetric channel fading coefficients has been characterized based on the ergodic interference alignment [44]. Further more, its inner bound is characterized only by “local” rate constraints associated with each node, which makes it feasible to be served as building blocks for large networks.

V. ILLUSTRATIVE EXAMPLES

In this section we illustrate our capacity bounding models by several coupled noisy networks and compare the capacity inner and outer bounds obtained based on our bounding models with some benchmarks. Given a coupled noisy network \mathcal{N} , we first apply the channel decoupling method proposed in Sec. IV-A to decompose the coupled network into decoupled MACs and BCs. We then construct an upper bounding model $\mathcal{C}_{u,i}$ following the procedure described in Sec. IV-B and a lower bounding model $\mathcal{C}_{l,i}$ as in Sec. IV-C. As there are more than one upper (resp. lower) bounding model for every MAC/BC, each of such combinations will result in a noiseless upper bounding model $\mathcal{C}_{u,i}$ (resp. lower bounding model $\mathcal{C}_{l,i}$), whose capacity region serves as a capacity outer (resp. inner) bound for the original noisy network \mathcal{N} . We then take the intersection of all the capacity outer bounds, one for each $\mathcal{C}_{u,i}$, to obtain the final (and tighter) outer bound,

$$\mathcal{E}(\mathcal{N}) \subseteq \bigcap_i \mathcal{E}(\mathcal{C}_{u,i}), \quad (88)$$

where $\mathcal{E}(\cdot)$ denotes the capacity region of the corresponding network. For the inner bound, we compute the achievable rate region for each lower bounding model $\mathcal{C}_{l,i}$ and then take the convex hull of all the achievable rate regions to create the final (and tighter) inner bound (with abuse of notation),

$$\bigcup_i \mathcal{E}(\mathcal{C}_{l,i}) \subseteq \mathcal{E}(\mathcal{N}). \quad (89)$$

A. The Smallest Coupled Network: the Relay Channel

We first look at the smallest (in size) coupled network — the classical 3-node Gaussian relay channel — as illustrated in Fig. 7(a), which can be modelled as

$$\begin{aligned} Y &= \sqrt{\gamma_{sd}}X + \sqrt{\gamma_{rd}}X_r + Z, \\ Y_r &= \sqrt{\gamma_{sr}}X + Z_r, \end{aligned}$$

where γ_{sd} , γ_{sr} , and γ_{rd} are effective link SNRs, Z and Z_r are independent Gaussian noise with zero mean and unit variance, and X and X_r are transmitting signals subject to unit average power constraint. The lower bounding model has two types: we use the topology shown in Fig. 7(c) if the source-destination link is better than the source-relay link, otherwise Fig. 7(d) is chosen.

The upper bounding model (R_d, R_{d1}, R_{d2}) for the decoupled MAC can be constructed following the technique developed in Sec. III-A with link SNRs γ_{sd} and γ_{rd} . The upper bounding model (R_s, R_{l1}, R_{l2}) for the decoupled BC can be constructed following the technique developed in Sec. III-B but with adjusted link SNRs γ_{sd}/α and γ_{sr} . The optimal noise partition parameter α is uniquely determined by the convex

¹³This assumption always holds as we can set $\gamma_{ik} = 0$ for all $k \notin D_i$, and change labels when necessary.

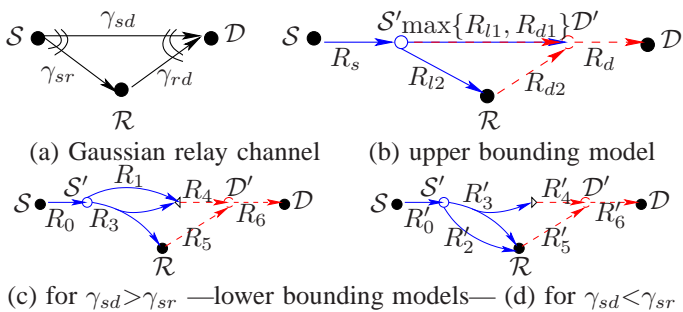


Fig. 7. The three-node Gaussian relay channel (a), its upper bounding model (b), and lower bounding models for the scenario when the source-destination link has stronger (c) or weaker (d) channel gain compared to the source-relay link

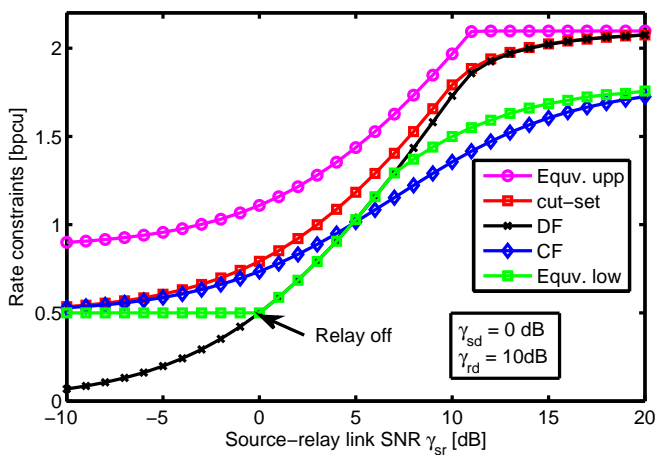


Fig. 8. Upper and lower bounds on the capacity of a Gaussian relay channel with source-destination link SNR $\gamma_{sd} = 0$ dB and relay-destination link SNR $\gamma_{rd} = 10$ dB. Without resorting to source-relay cooperation, our equivalence lower bound demonstrates the general behavior of both CF (strong/weak γ_{sr}) and DF (medium γ_{sr}) while remaining a single bounding technique.

optimization problem defined in (81), whose solution for this special case can be solved analytically,¹⁴

$$\alpha = \frac{\sqrt{\gamma_{sd}(1 + \gamma_{rd})}}{\sqrt{\gamma_{rd}(1 + \gamma_{sr} + \gamma_{sd})} + \sqrt{\gamma_{sd}(1 + \gamma_{rd})}}. \quad (90)$$

The connection between the auxiliary nodes S' and D' has two parallel rate constraints— R_{l1} imposed by the decoupled BC and R_{d1} by the MAC—which results in the rate constraint $\max\{R_{l1}, R_{d1}\}$ as shown in Fig. 7(b).

In Fig. 8 we evaluate the upper and lower bounds obtained from our bounding models with respect to varying source-relay link SNR γ_{sr} , and compare them to three benchmarks developed in [29]: the cut-set upper bound, the decode-and-forward (DF) lower bound, and the compress-and-forward (CF) lower bound. Without resorting to source-relay cooperation, our equivalence lower bound outperforms CF and only suffers a loss of 0.3 bits per channel use compared to DF when the source-relay link is strong. When the source-relay link is weak, it approaches the capacity and outperforms DF by turning off the “less capable” relay node (when $\gamma_{sr} \leq \gamma_{sd}$). Note that our equivalence lower bound has the general behavior of both

¹⁴Following the same process as in Appendix D but focusing only on equations defined by (120).

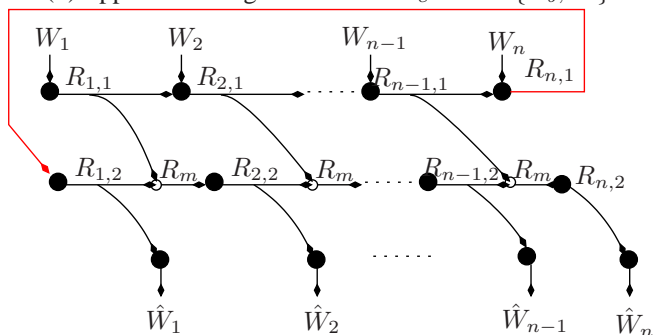
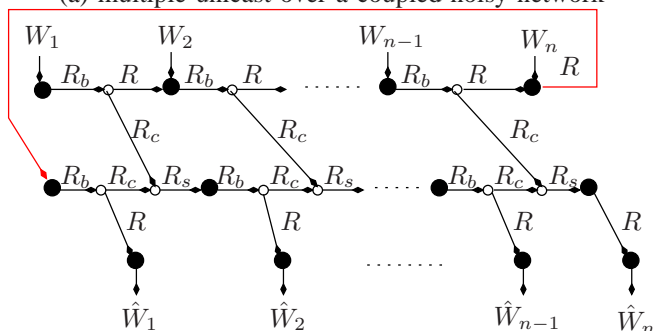
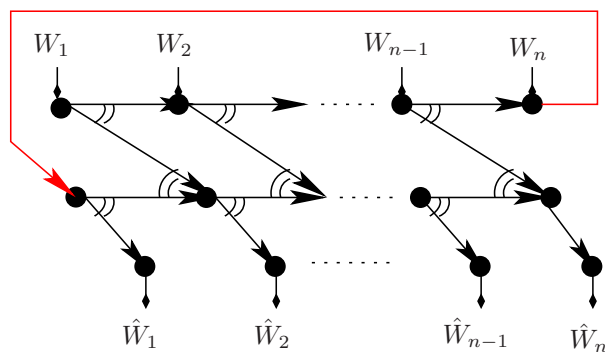


Fig. 9. Multiple unicast transmission over a coupled noisy network (a) where the channel in red color is the bottleneck. Assuming all channels are Gaussian with identical link SNR γ , the upper bounding model (b) has only point-to-point bit pipes and the lower bounding model (c) also contains point-to-points bit pipes (hyper-arcs) due to the broadcast transmission.

CF (strong/weak γ_{sr}) and DF (medium γ_{sr}). Our equivalence upper bound, which assumes perfect source-relay cooperation and relay-destination joint decoding, has a gap of around 0.4 bits from the cut-set upper bound when γ_{sr} is small and the gap vanishes when γ_{sr} becomes large.

B. Multiple Unicast over a Layered Noisy Network

In Fig. 9(a) we focus on a layered multiple-unicast noisy network where n source-destination pairs are assisted by n intermediate relaying nodes. It is a modified version of [4, Fig. 3]¹⁵ by replacing the orthogonal transmissions to the relaying nodes with MACs to formulate a coupled network. Assuming all transmission channels are identical and all unicast rates are the same, the channel in red color is the

¹⁵The network of [4, Fig. 3] is obtained from the multiple-unicast network in [43, Fig. 1] which consists of point-to-point bit pipes only.

TABLE II

TRANSMISSION SCHEME WITH $n = 4$ WHERE SOURCE NODE \mathcal{S}_i UNICASTS MESSAGES W_i^b , $b=1, \dots, B$, TO DESTINATION NODE \mathcal{D}_i OVER $(n \cdot B+1)$ TRANSMISSION BLOCKS. $W_i^0 = \emptyset$ BY DEFAULT INDICATES NO TRANSMISSION.

$t = \setminus \text{TX}$	\mathcal{S}_1	\mathcal{S}_2	\mathcal{S}_3	\mathcal{S}_4	\mathcal{R}_1	\mathcal{R}_2	\mathcal{R}_3	\mathcal{R}_4
$4(b-1)+1$	$W_1^b W_2^b$	$W_3^b W_4^b$	$W_1^{b-1} W_2^{b-1}$	$W_3^{b-1} W_4^{b-1}$	$W_1^{b-1} W_2^{b-1}$	$W_3^{b-1} W_4^{b-1}$	$W_1^{b-1} W_2^{b-1}$	$W_3^{b-1} W_4^{b-1}$
$4(b-1)+2$	\emptyset	W_1^b	W_2^b	W_3^b	W_4^b	\emptyset	\emptyset	\emptyset
$4(b-1)+3$	\emptyset	\emptyset	W_1^b	W_2^b	W_3^b	W_4^b	\emptyset	\emptyset
$4(b-1)+4$	\emptyset	\emptyset	\emptyset	W_1^b	W_2^b	W_3^b	W_4^b	\emptyset

bottleneck. If all channels are Gaussian with link SNR γ , we can construct an upper bounding model as shown in Fig. 9(b) by first performing channel decoupling as described in Sec. IV-A, and then substituting the upper bounding models developed in Sec. III-B to replace BCs at source nodes by $\mathcal{C}_{u,BC,a} = (R_b, R, R_b)$, BCs at intermediate relaying nodes by $\mathcal{C}_{u,BC,b} = (R_b, R_b, R)$, and MACs by $\mathcal{C}_{u,MAC,new}(\alpha) = (R_s, R', R')$, where

$$R = \frac{1}{2} \log(1 + \gamma), \quad (91)$$

$$R_b = \frac{1}{2} \log(1 + 3\gamma), \quad (92)$$

$$R' = \frac{1}{2} \log\left(1 + \frac{\gamma}{(1-\alpha)/2}\right), \quad (93)$$

$$R_s = \frac{1}{2} \log\left(1 + \frac{4\gamma + 1 - \alpha}{\alpha}\right). \quad (94)$$

Note that although the value of R_s and R_c in Fig. 9(b) may change by varying $\alpha \in [0, 1]$, the red-color link of capacity R is always the bottleneck, and therefore the symmetric-rate unicast capacity is upper bounded by R/n . This is actually the capacity as all the source nodes can successfully transmit B packets each over $(B \cdot n + 1)$ transmission blocks, which leads to a rate

$$\frac{B \cdot R}{B \cdot n + 1} = \frac{R}{n + 1/B} \rightarrow \frac{R}{n}, \text{ when } B \rightarrow \infty.$$

We illustrate the transmission scheme in Table II by an example with $n = 4$.

The lower bounding model in Fig. 9(c) contains point-to-points bit pipes (hyper-arcs) of rate $R_{i,k} \leq R$, for $i = 1, \dots, n$, $k=1, 2$. By forcing successful decoding at MACs, we will have the following constraints

$$R_{i,1} + R_{i,2} \leq R_m \triangleq \frac{1}{2} \log(1 + 2\gamma), \forall i = 1, \dots, n-1. \quad (95)$$

Therefore we can conclude from the lower bounding model that a rate R_l is achievable if for all $i = 1, \dots, n$,

$$iR_l \leq R_{i,1}, \quad (96)$$

$$(n - i + 1)R_l \leq R_{i,2}. \quad (97)$$

After applying the MAC constraint (95), we have

$$R_l = \min\left\{\frac{R}{n}, \frac{R_m}{n+1}\right\} \quad (98)$$

$$= \begin{cases} \frac{R}{n}, & \text{if } \gamma < \frac{1+\sqrt{5}}{2} \text{ or } n \geq \frac{\log(1+\gamma)}{\log(1+\gamma/(1+\gamma))}, \\ \frac{R_m}{n+1}, & \text{otherwise.} \end{cases} \quad (99)$$

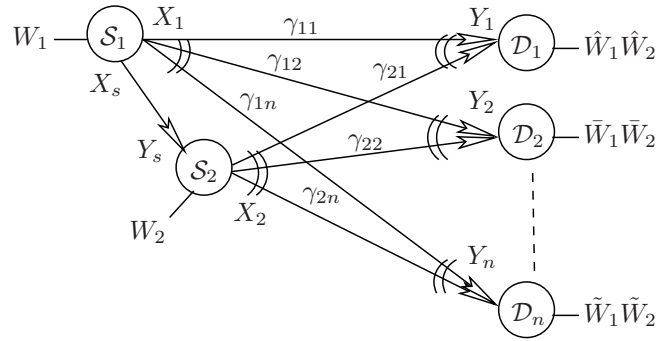


Fig. 10. Two source nodes \mathcal{S}_1 and \mathcal{S}_2 multicast W_1 and W_2 respectively to all destinations $\{\mathcal{D}_i : i = 1, \dots, n\}$ through Gaussian channels, where γ_{ji} denotes the SNR of the link from \mathcal{S}_j to \mathcal{D}_i . The link $(X_s \rightarrow Y_s)$ from \mathcal{S}_1 to \mathcal{S}_2 is a Q -ary symmetric channel orthogonal to all the other Gaussian channels.

Therefore the lower bounding models can provide a rate equals the capacity R/n when the the SNR γ is small or when the number of nodes is large.

C. Multiple Multicast over a Wireless Relay Network

We now illustrate the construction of bounding models for a multiple multicast relay network shown in Fig. 10, where two source nodes \mathcal{S}_1 and \mathcal{S}_2 multicast information W_1 at rate R_1 and W_2 at rate R_2 , respectively, to all destinations $\{\mathcal{D}_i : i = 1, \dots, n\}$ over Gaussian channels. The effective SNRs of these Gaussian channels are

$$\begin{aligned} \gamma_{1k} &= P - \frac{k}{n} \Delta_P, \\ \gamma_{2k} &= P + \frac{k}{n} \Delta_P, \end{aligned} \quad (100)$$

where $P > \Delta_P > 0$ are parameters such that

$$\gamma_{2n} > \dots > \gamma_{21} > \gamma_{11} > \dots > \gamma_{1n}. \quad (101)$$

The transmission of \mathcal{S}_1 is aided by \mathcal{S}_2 via a Q -ary symmetric channel $(X_s \rightarrow Y_s)$ such that for all $m, k \in \{0, 1, \dots, Q-1\}$

$$Pr(Y_s = m | X_s = k) = \begin{cases} 1 - \xi, & \text{if } m = k, \\ \frac{\xi}{Q-1}, & \text{if } m \neq k. \end{cases} \quad (102)$$

We can first decompose the original network into a point-to-point channel, two decoupled BCs originating from \mathcal{S}_1 and \mathcal{S}_2 , and n decoupled MACs ending at each destination node, and then construct upper and lower bounding models as described in Sec IV. An illustration of the resulting lower bounding model for $n = 3$ is presented in Fig. 11, where the rate constraints of poin-to-point(s) bit pipes are determined following the process in Sec. IV-C. From Fig. 11 we can see that multicast of W_2 can only be achieved via the hyper-arc of rate R_7 , while multicast of W_1 can be achieved either via the hyper-arc of rate R'_7 , or via the collaboration with \mathcal{S}_2 at rates $\min\{R'_3, R_4\}$ and/or $\min\{R'_1, R_6\}$. The collaboration from \mathcal{S}_2 is subject to the rate constraint C_{12} which is the capacity of the Q -array symmetric channel from \mathcal{S}_1 to \mathcal{S}_2 .

The bounds on sum rate obtained from upper and lower bounding networks with respect to varying channel quality have been illustrated in Fig. 12 for a scenario with $n = 10$

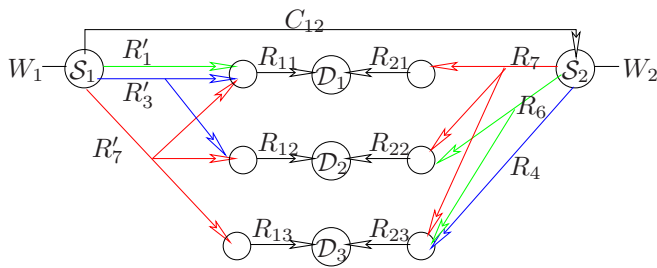


Fig. 11. Lower bounding model for the scenario with $n = 3$ destinations where C_{12} is the channel capacity of the Q -ary symmetric channel ($X_s \rightarrow Y_s$). R'_3 and R'_7 are the rates of hyper-arcs from \mathcal{S}_1 to $\{\mathcal{D}_1\mathcal{D}_2\}$ and $\{\mathcal{D}_1\mathcal{D}_2\mathcal{D}_3\}$, respectively, and R_6 denotes the multicast rate from \mathcal{S}_2 to $\{\mathcal{D}_2\mathcal{D}_3\}$. Rate constraints R_{sd} , $s = 1, 2$ and $d = 1, 2, 3$, come from the lower bounding models of MACs.

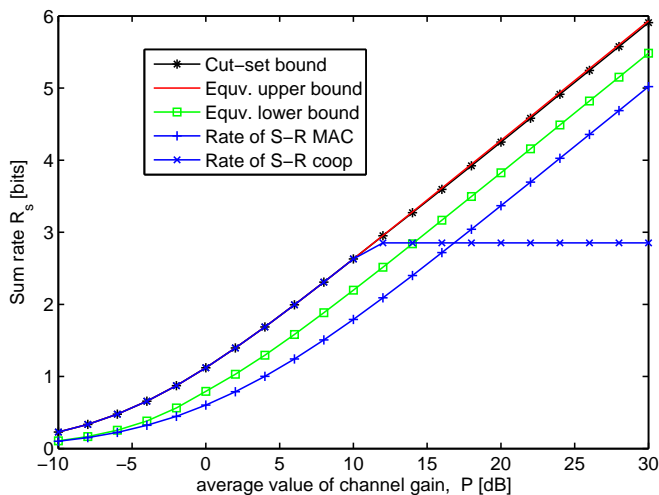


Fig. 12. Bounds on the sum rate for the scenario with 10 destinations, $\delta_P/P = -3$ dB, and the Q -ary symmetric channel ($X_s \rightarrow Y_s$) with $Q = 8$ and $\xi = 0.1$.

destinations. The Q -ary symmetric channel ($X_s \rightarrow Y_s$) has parameters $Q = 8$ and $\xi = 0.1$, which results in a capacity of $C_{12} = 2.85$ bits per channel use [bpcu]. We also plot three benchmarks as references: the rate achieved by transmitting identical signals from \mathcal{S}_1 and \mathcal{S}_2 (denoted by “S1-S2 coop”), the rate achieved by transmitting independent signals from \mathcal{S}_1 and \mathcal{S}_2 (denoted by “S1-S2 MAC”), and the cut-set upper bound following the method developed in [29]¹⁶. Our upper bound obtained from noiseless bounding networks is very good¹⁷ and it even approaches the capacity (meeting the lower bound provided by \mathcal{S}_1 - \mathcal{S}_2 cooperation) in low to medium SNR regions. Our lower bounding models discard the possibility of source cooperation and therefore suffers some performance degradation (less than 0.4 bits¹⁸ from the capacity). In high

¹⁶In [29] the cut-set bound is obtained by starting from multi-letter expressions and then combining various inequalities, average power constraints, and some “properly” chosen auxiliary random variables. Here “properly” is to highlight the fact that it is a kind of art to decide when and where to introduce auxiliary random variables to quantify the possible correlation among transmitting signals, since only proper choice leads to nice upper bounds. See [30]–[32] for extensions of the method developed in [29].

¹⁷In the sense that the gap from cut-set bound is negligible.

¹⁸As P and n increase, the gap from cut-set bound converges to a constant that depends only on Δ_P/P .

SNR region, it outperforms the two benchmarks since our lower bounding models can make use of the overhead messages to increase the multicast rate of W_1 : extra bits of W_1 can be transmitted via the collaboration with \mathcal{S}_2 at rate

$$\Delta_{R1} = \min\{R'_3, R_4\} + \min\{R'_1, R_6\}, \quad (103)$$

if such operation is permitted by the link from \mathcal{S}_1 to \mathcal{S}_2 , i.e., when $R_4 + R_6 < C_{12}$.

VI. SUMMARY

In this work we have presented capacity upper and lower bounding models for wireless networks, where the upper bounding models consist of only point-to-point bit pipes while the lower bounding models also contains point-to-points bit pipes (hyper-arcs). We have extended the bounding models for two-user MACs/BCs to many-user scenarios and established a constant additive gap between upper and lower bounding models. For networks with coupled links, we have proposed a channel decoupling method to decompose coupled networks into decoupled MACs and BCs, and proposed strategies to construct step-by-step upper and lower bounding models for the originally coupled networks. We have demonstrated by examples that the gap between the resulting upper and lower bounds is usually not large, and the upper/lower bound can approach capacity in some setups. The proposed methods for constructing upper and lower bounding models, effective and computationally efficient, can be easily extended to large networks with complexity grows linearly with the number of nodes. They therefore, combined with methods calculating the capacity of noiseless networks, provide additional powerful tools for characterizing the capacity region of general wireless networks.

APPENDIX A

OPTIMAL NOISE PARTITIONING FOR GAUSSIAN MACS

Following the Lagrangian method [33], the optimal noise partitioning for the optimization problem (36) can be obtained by taking partial derivatives of its Lagrangian

$$L = \sum_i \log(1 + \gamma_i/\alpha_i) + \mu^{-1} \left(\sum_i \alpha_i - (1 - \alpha) \right), \quad \mu > 0, \quad (104)$$

with respect to α_i , $i = 1, \dots, m$, and setting them to zero. Denoting α_i^* the optimal noise power for α_i , we have

$$(\alpha_i^*)^2 + \gamma_i \alpha_i^* - \gamma_i \mu = 0, \quad (105)$$

which leads to (omitting the negative root as $\alpha_i^* > 0$)

$$\alpha_i^* = \frac{\sqrt{\gamma_i(\gamma_i + 4\mu)} - \gamma_i}{2}. \quad (106)$$

The exact value of μ is determined by the condition $\sum_{i=1}^m \alpha_i = 1 - \alpha$, which yields (37).

APPENDIX B
PROOF OF LEMMA 3

The upper bound is obtained by contradiction. Assuming $\mu > \frac{1-\alpha}{m} + \frac{(1-\alpha)^2}{m^2} \frac{1}{\min_i \gamma_i}$, the LHS of (37) is evaluated as follows

$$\begin{aligned} \text{LHS} &> \frac{1}{2} \sum_{j=1}^m \left(\sqrt{\left(\gamma_j + \frac{1-\alpha}{m/2} \right)^2 + \frac{(1-\alpha)^2}{m^2} \left(\frac{\gamma_j}{\min_i \gamma_i} - 1 \right)} - \gamma_j \right) \\ &\geq \frac{1}{2} \sum_{j=1}^m \left(\sqrt{\left(\gamma_j + \frac{1-\alpha}{m/2} \right)^2} - \gamma_j \right) \\ &= 1 - \alpha, \end{aligned} \quad (107)$$

which contradicts to the equality constraint stated in (37). Therefore we have

$$\mu \leq \frac{1-\alpha}{m} + \frac{(1-\alpha)^2}{m^2} \frac{1}{\min_i \gamma_i}, \quad (108)$$

where the equality holds if and only if $\gamma_j = \min_i \gamma_i$ for all $j=1, \dots, m$, i.e., when $\gamma_1 = \dots = \gamma_m$.

The lower bound is obtained as follows. From (37) we have

$$\left(2(1-\alpha) + \sum_i \gamma_i \right)^2 = \left(\sum_i \sqrt{\gamma_i(\gamma_i + 4\mu)} \right)^2 \quad (109)$$

$$\leq \left(\sum_i \gamma_i \right) \left(4m\mu + \sum_i \gamma_i \right) \quad (110)$$

$$= 4m\mu \sum_i \gamma_i + \left(\sum_i \gamma_i \right)^2, \quad (111)$$

where the inequality in (110) is due to Cauchy-Schwarz inequality with equality holds if and only if $\gamma_1 = \dots = \gamma_m$. By expanding the LHS and removing common items at both sides, we can easily obtain the lower bound.

APPENDIX C
PROOF OF LEMMA 4

From (34) it is straightforward to observe that $R_s(\alpha)$ is a monotonously decreasing function with respect to α , with its minimum

$$R_s(\alpha < 1) > R_s(\alpha = 1) = R_{MAC} \triangleq \frac{1}{2} \log \left(1 + \left(\sum_{i=1}^m \sqrt{\gamma_i} \right)^2 \right). \quad (112)$$

Therefore we only need to prove $\sum_{i=1}^m R_i(\alpha) > R_{MAC}$.

From (35) and (37) it is easy to see that $R_i(\alpha)$ is a monotonously increasing function with respect to $\alpha \in [0, 1)$, which leads to

$$\sum_{i=1}^m R_i(\alpha > 0) > \sum_{i=1}^m R_i(\alpha = 0). \quad (113)$$

On the other hand, we have

$$\sum_{i=1}^m R_i(\alpha = 0) = \sum_{i=1}^m \frac{1}{2} \log \left(1 + \frac{\gamma_i}{\alpha_i} \right) \quad (114)$$

$$> \frac{1}{2} \log \left(1 + \sum_{i=1}^m \frac{\gamma_i}{\alpha_i} \right) \quad (115)$$

$$\geq \frac{1}{2} \log \left(1 + \min_{x_i > 0; \sum_{i=1}^m x_i = 1} \sum_{i=1}^m \frac{\gamma_i}{x_i} \right) \quad (116)$$

$$= \frac{1}{2} \log \left(1 + \left(\sum_{i=1}^m \sqrt{\gamma_i} \right)^2 \right) \quad (117)$$

$$= R_{MAC}, \quad (118)$$

where (117) holds by the optimal solution $x_i^* = \sqrt{\gamma_i} / (\sum_j \sqrt{\gamma_j})$. Hence we have proved the lemma.

APPENDIX D
NOISE PARTITION FOR GAUSSIAN CHANNEL DECOUPLING

Let

$$L = \sum_{i=1}^n \log \left(1 + \sum_{j=1}^m \frac{\gamma_{i,j}}{\alpha_{i,j}} \right) + \sum_{j=1}^m \lambda_j \left(\sum_{i=1}^n \alpha_{i,j} - 1 \right), \quad (119)$$

be the Lagrangian, by taking partial derivative of L w.r.t. $\alpha_{i,j}$ and setting them to zero, we get

$$\frac{\gamma_{i,j}}{\alpha_{i,j}^2} = \lambda_j \left(1 + \sum_{k=1}^m \frac{\gamma_{i,k}}{\alpha_{i,k}} \right). \quad (120)$$

By introducing auxiliary variables

$$\mu_i = 1 + \sum_{j=1}^m \frac{\gamma_{i,j}}{\alpha_{i,j}}, \quad \forall i \in \{1, \dots, n\}, \quad (121)$$

we can derive from (120) the following equations

$$\alpha_{i,j} = \frac{\sqrt{\gamma_{i,j}}}{\sqrt{\lambda_j} \sqrt{\mu_i}}, \quad (122)$$

$$\frac{\gamma_{i,j}}{\alpha_{i,j}} = \sqrt{\gamma_{i,j}} \sqrt{\lambda_j} \sqrt{\mu_i}, \quad (123)$$

$$\sqrt{\lambda_j} = \sum_{i=1}^n \frac{\sqrt{\gamma_{i,j}}}{\sqrt{\mu_i}}, \quad (124)$$

$$\mu_i = 1 + \sqrt{\mu_i} \sum_{j=1}^m \sqrt{\gamma_{i,j}} \sqrt{\lambda_j}, \quad (125)$$

$$\sqrt{\mu_i} = \frac{1}{2} \left(\sqrt{\left(\sum_{j=1}^m \sqrt{\gamma_{i,j}} \sqrt{\lambda_j} \right)^2 + 4} + \sum_{j=1}^m \sqrt{\gamma_{i,j}} \sqrt{\lambda_j} \right), \quad (126)$$

where (124) comes from (122) and the fact that $\sum_{i=1}^n \alpha_{i,j} = 1$, (125) is obtained by substituting (123) into (121), and (126) is the unique feasible solution to (125). Therefore the equivalent SNRs $\frac{\gamma_{i,j}}{\alpha_{i,j}}$ for decoupled BCs are uniquely determined by (123) where the optimal value of μ_i and λ_j can be easily obtained by iterating (124) and (126). The convergence to the

global optimum is guaranteed by observing the fact that λ_j is a monotonically decreasing function of $\{\mu_i : \forall i\}$ via (124) and μ_i is a monotonically increasing function of $\{\lambda_j : \forall j\}$, via (126).

REFERENCES

- [1] R. Koetter, M. Effros, and M. Médard, "A theory of network equivalence—part I: point-to-point channels," *IEEE Transactions on Information Theory*, vol. 57, pp. 972–995, Feb. 2011.
- [2] R. Koetter, M. Effros, and M. Médard, "A theory of network equivalence, part II," 2010, arXiv:1007.1033.
- [3] M. Effros, "On capacity outer bounds for a simple family of wireless networks," in *Proceedings Information Theory and Applications Workshop (ITA)* Feb. 2010.
- [4] M. Effros, "Capacity Bounds for Networks of Broadcast Channels," in *Proceedings IEEE International Symposium on Information Theory (ISIT)*, Jun. 2010.
- [5] N. Fawaz and M. Médard, "A Converse for the Wideband Relay Channel with Physically Degraded Broadcast," in *Proceedings IEEE Information Theory Workshop (ITW)*, Oct. 2011.
- [6] F. P. Calmon, M. Médard, and M. Effros, "Equivalent models for multi-terminal channels," in *Proceedings IEEE Information Theory Workshop (ITW)*, Oct. 2011.
- [7] C. E. Shannon, "A mathematical theory of communication," *Bell System Technical Journal*, vol. 27, pp. 379–423 and pp. 623–656, 1948.
- [8] S. P. Borade, "Network information flow: limits and achievability," in *Proceedings IEEE International Symposium on Information Theory (ISIT)*, Jul. 2002.
- [9] L. Song, R. W. Yeung, and N. Cai, "A separation theorem for single-source network coding," *IEEE Transactions on Information Theory*, vol. 52, pp. 1861–1871, May 2006.
- [10] T. M. Cover and J. A. Thomas, *Elements of Information Theory*. New York: Wiley, 2006.
- [11] B. Hassibi and S. Shadbakht, "Normalized entropy vectors, network information theory and convex optimization," in *Proceedings IEEE Information Theory Workshop (ITW)*, Jul. 2007.
- [12] C. Bennett, P. Shor, J. Smolin, and A. Thapliyal, "Entanglement-assisted capacity of a quantum channel and the reverse Shannon theorem," *IEEE Transactions on Information Theory*, vol. 48, pp. 2637–2655, Oct. 2002.
- [13] P. W. Cuff, H. H. Permuter, and T. M. Cover, "Coordination Capacity," *IEEE Transactions on Information Theory*, vol. 56, pp. 4181–4206, Sep. 2010.
- [14] C. Tian, J. Chen, S. Diggavi, and S. Shamai (Shitz), "Optimality and approximate optimality of source-channel separation in networks," *IEEE Transactions on Information Theory*, vol. 60, pp. 904–918, Feb. 2014.
- [15] S. Jalali and M. Effros, "Separation of source-network coding and channel coding in wireline networks," ArXiv:1110.3559.
- [16] A. R. Lehman and E. Lehman, "Complexity classifications of network information flow problems," in *Proceedings 41st Annual Allerton Conference on Communication, Control, and Computing*, Sep. 2003.
- [17] T. Chan and A. Grant, "Dualities between entropy functions and network codes," *IEEE Transactions on Information Theory*, vol. 49, pp. 3129–3139, Oct. 2008.
- [18] R. Koetter and M. Médard, "An algebraic approach to network coding," *IEEE/ACM Transactions on Networking*, vol. 11, pp. 782–795, Oct. 2003.
- [19] L. Song, R. W. Yeung, and N. Cai, "Zero-error network coding for acyclic networks," *IEEE Transactions on Information Theory*, vol. 49, pp. 3129–3139, Jul. 2003.
- [20] N. Harvey, R. Kleinberg, and A. R. Lehman, "On the capacity of information networks," *IEEE Transactions on Information Theory*, vol. 52, pp. 2345–2364, Jun. 2006.
- [21] X. Yan, J. Yang, and Z. Zhang, "An outer bound for multisource multisink network coding with minimum cost consideration," *IEEE Transactions on Information Theory*, vol. 52, pp. 2373–2385, Jun. 2006.
- [22] G. Kramer and S. Savari, "Edge-cut bounds on network coding rates," *Journal of Network and Systems Management*, vol. 14, pp. 49–67, Mar. 2006.
- [23] A. Subramanian and A. Thangaraj, "Path gain algebraic formulation for the scalar linear network coding problem," *IEEE Transactions on Information Theory*, vol. 56, pp. 4520–4531, Sep. 2010.
- [24] S. Kamath and P. Viswanath, "An information-theoretic meta-theorem on edge-cut bounds," in *Proceedings IEEE International Symposium on Information Theory (ISIT)*, Jul. 2012.
- [25] A. S. Avestimehr, S. N. Diggavi, and D. N. C. Tse, "Wireless network information flow: a deterministic approach," *IEEE Transactions on Information Theory*, vol. 57, pp. 1872–1905, Apr. 2011.
- [26] I. Marić, A. Goldsmith, and M. Médard, "Multihop analog network coding via amplify-and-forward: the high SNR regime," *IEEE Transactions on Information Theory*, vol. 58, pp. 793–803, Feb. 2012.
- [27] S. Kannan, A. Raja, and P. Viswanath, "Local phy + global flow: a layering principle for wireless networks," in *Proceedings IEEE International Symposium on Information Theory (ISIT)*, Aug. 2011.
- [28] S. Kannan and P. Viswanath, "Capacity of multiple unicast in wireless networks: a polymatroidal approach," *IEEE Transactions on Information Theory*, vol. 60, pp. 6303–6328, Oct. 2014.
- [29] T. M. Cover and A. El Gamal, "Capacity theorems for the relay channel," *IEEE Transactions on Information Theory*, vol. 25, pp. 572–584, Sep. 1979.
- [30] J. Du, M. Xiao, and M. Skoglund, "Capacity bounds for backhaul-supported wireless multicast relay networks with cross-links," in *Proceedings IEEE International Conference on Communications (ICC)*, Jun. 2011.
- [31] J. Du, M. Xiao, and M. Skoglund, "Cooperative network coding strategies for wireless relay networks with backhaul," *IEEE Transactions on Communications*, vol. 59, pp. 2502–2514, Sep. 2011.
- [32] J. Du, M. Xiao, M. Skoglund, and M. Médard, "Wireless multicast relay networks with limited-rate source-conferencing," *IEEE Journal on Selected Areas in Communications*, vol. 31, pp. 1390–1401, Aug. 2013.
- [33] S. Boyd and L. Vandenberghe, *Convex Optimization*, Cambridge University Press, 2004.
- [34] A. El Gamal and Y.-H. Kim, *Network Information Theory*. Cambridge University Press, 2011.
- [35] S. W. Ho and R. W. Yeung, "On information divergence measures and a unified typicality," *IEEE Transactions on Information Theory*, vol. 56, pp. 5893–5905, Dec. 2010.
- [36] Y. Oohama, "The rate-distortion function for the quadratic Gaussian CEO problem," *IEEE Transactions on Information Theory*, vol. 44, pp. 1057–1070, May 1998.
- [37] J. Jeon, "A generalized typicality for abstract alphabets," arXiv:1401.6728v3, May 2014.
- [38] E. C. Song, P. Cuff, and H. V. Poor, "The likelihood encoder for lossy compression," arXiv:1408.4522, Aug. 2014.
- [39] P. Cuff, "Distributed channel synthesis," *IEEE Transactions on Information Theory*, vol. 59, pp. 7071–7096, Nov. 2013.
- [40] A. Wyner, "The common information of two dependent random variables," *IEEE Transactions on Information Theory*, vol. 21, pp. 163–179, Mar. 1975.
- [41] M. Costa, "Writing on dirty paper," *IEEE Transactions on Information Theory*, vol. 29, pp. 439–441, May 1983.
- [42] D. Traskov, M. Heindlmaier, M. Médard, and R. Koetter, "Scheduling for network coded multicast," *IEEE/ACM Transactions on Networking*, vol. 20, pp. 1479–1488, Oct. 2012.
- [43] N. Harvey and R. Kleinberg, "Tighter cut-set bounds for k -pairs communication problems," in *Proceedings 43rd Annual Allerton Conference on Communication, Control, and Computing*, Sep. 2005.
- [44] B. Nazer, M. Gastpar, S. A. Jafar, and S. Vishwanath, "Ergodic interference alignment," in *Proceedings IEEE International Symposium on Information Theory (ISIT)*, Jul. 2009.